https://doi.org/10.5194/acp-2021-429
Preprint. Discussion started: 7 September 2021

Atmospheric Chemistry and Physics Discussions

Development and evolution of an anomalous Asian dust event across Europe in March 2020

Laura Tositti[1], Erika Brattich[2], Claudio Cassardo[3], Pietro Morozzi[1], Alessandro Bracci[2], Angela Marinoni[4], Silvana Di Sabatino[2], Federico Porcù[2], Alessandro Zappi[1]

[1] Department of Chemistry "G. Ciamician", Alma Mater Studiorum University of Bologna, Via F. Selmi, 2, 40126 Bologna (Italy)

[2] Department of Physics and Astronomy "Augusto Righi", Alma Mater Studiorum University of Bologna Viale Berti Pichat 6/2, 40127 Bologna (Italy)

[3] Department of Physics, via P. Giuria 1, 10125 Torino (Italy)

[4] National Research Counsil of Italy, Institute of Atmospheric Sciences and Climate (CNR-ISAC), Via P. Gobetti, 101, 40129 Bologna (Italy)

Correspondence to: Laura Tositti (laura.tositti@unibo.it)

https://doi.org/10.5194/acp-2021-429
Preprint. Discussion started: 7 September 2021

Atmospheric Chemistry and Physics Discussions

Abstract. This paper concerns an in-depth analysis of an exceptional incursion of mineral dust over Southern Europe in late March 2020. This event was associated with an anomalous circulation pattern leading to several days of PM_{10} exceedances in connection with a dust source located in Central Asia a rare source of dust for Europe, more frequently affected by dust outbreaks from the Sahara desert. The synoptic meteorological configuration was analyzed in detail, while aerosol evolution during the transit of the dust cloud over Northern Italy was assessed at high time resolution by means of optical particle counting at three stations, namely Bologna, Trieste, and Mt. Cimone allowing to reveal transport timing among the three locations. Back-trajectory analyses supported by AOD (Aerosol Optical Depth) maps allowed to locate the mineral dust source area in the Aralkum region. The event was therefore analyzed through the observation of particle number size distribution with the support of chemical composition analysis. It is shown that PM_{10} exceedance recorded is associated with a large fraction of coarse particles in agreement with mineral dust properties. Both in-situ number size distribution and vertical distribution of the dust plume were cross-checked by Lidar Ceilometer and AOD data from two nearby stations, showing that the dust plume, differently from those originated in the Sahara desert, traveled close to the ground up to a height of about 2 km. The limited mixing layer height caused by high concentrations of absorbing and scattering aerosols caused the mixing of mineral dust with other locally-produced ambient aerosols, thereby potentially increasing its morbidity effects.

https://doi.org/10.5194/acp-2021-429
Preprint. Discussion started: 7 September 2021

Atmospheric Chemistry and Physics Discussions

1 Introduction

Mineral dust originating in desert regions is one of the main components of the ambient aerosol affecting air quality and human health, cloud formation, ocean ecosystems, and climate (Knippertz and Stuut, 2014; Schepanski, 2018). Despite its significance, mineral dust still represents one of the largest uncertainties in climate modeling (Adebiyi and Kok, 2020; IPCC Working Group I, 2013). Mineral dust is often transported at a large scale influencing vast continental and ocean areas (Barkan and Alpert, 2010). The most immediate effect of mineral dust in a specific area is the increase, sometimes dramatic, of particulate matter (PM) mass loading (Brattich et al., 2015a), mainly in the coarse fraction. Several studies also demonstrated that mineral dust can affect cloud processing (Bangert et al., 2012) and biogeochemical cycles of ecosystems (Okin et al., 2004). Numerous studies documented the health effects of mineral dust transport in various parts of the world (Domínguez-Rodríguez et al., 2021; Fubini and Fenoglio, 2007; Keil et al., 2016; Sajani et al., 2011; Stafoggia et al., 2016), owing to the conjunct impact of mineralogy, allergens, and pathogens (García-Pando et al., 2014). For these reasons, it is essential to study mineral dust composition in connection with its atmospheric path, source region, physicochemical properties, and modifications associated with environmental, climatic, and health issues.

The most important dust sources regions at the global scale are the North African Sahara region, the Arabian desert, the central Asia desert, the Dasht-e Margo (the desert region between Pakistan, Iran, and Afghanistan), the Great Basin (USA), the Kalahari desert (Southern Africa), and the central Australia deserts (Calidonna et al., 2020; Prospero et al., 2002; Washington et al., 2003). Recently another prominent source of mineral dust is drawing research interest, i.e., the semi-arid region between the Persian Gulf and the Caspian Sea. Several studies (Gholamzade Ledari et al., 2020; Kaskaoutis et al., 2018; Rashki et al., 2018) reported the transport of mineral dust originating in this region usually towards central and eastern Asia. With the purpose of evaluating the wind regime and dust activity in this region, a particular index, the Caspian Sea – Hindu Kush Index (CasHKI), has been introduced and studied in a long-term time series in previous studies (Kaskaoutis et al., 2018).

The primary source of desert dust reaching Southern Europe, including Italy, is the Sahara desert (Brattich et al., 2015a; Calidonna et al., 2020). In general, dust storms are more frequent in the spring-summer periods, while these are rare in the cold seasons (Brattich et al., 2015a; Duchi et al., 2016) to late winter (Fubini and Fenoglio, 2007; IPCC Working Group I, 2013). Saharan dust outbreaks are connected with several factors, among which the high temperatures, relatively intense winds, associated with cloud-free conditions, strong and perhaps increasing meridian gradients of pressure (African highs), while thermal convection promotes dust lifting and subsequent transport (Varga et al., 2013). Saharan dust outbreaks in Italy are mainly driven by pressure lows south of the peninsula, causing counterclockwise northward pulling of African desert air masses. While typically keeping its meridional character, this synoptic condition has been found to shift

https://doi.org/10.5194/acp-2021-429
Preprint. Discussion started: 7 September 2021


Atmospheric Chemistry and Physics Discussions

seasonally from the eastern in the spring to the western northern African coastal boundaries in the summer (Brattich et al., 2015a).

Differently from the vast literature on Saharan dust, the present work examines an outstanding mineral dust event whose characteristics are unprecedented to the best of our knowledge. The event described, indeed, concerns a singular and massive incursion of mineral dust reaching Europe from central Asia in late March 2020, a period marked by a series of peculiarities, not necessarily connected, such as an extensive, persistent, and intense eastern circulation, fairly infrequent at these latitudes, owing to basic dynamic constraints, the SARS COV-2 lockdown, and the concurrent, though seemingly out of context, large ozone hole in the Arctic (Manney et al., 2020).

The mineral dust incursion originating from the Caspian region widely bounced across the Italian media, as it led to PM_{10} concentration levels well above the EU air quality threshold, wedging over an area historically characterized by frequent and significant exceedances of this pollutant such as the Po valley (Tositti et al., 2014), mainly due to the accumulation of anthropogenic emissions. As a result, this contingency brought to harsh, though controversial connections between air quality across the regional airshed and the virus spread (Belosi et al., 2021; Prather et al., 2020).

Differently from the extensive literature on Saharan dust, as previously reminded, mineral dust from the Caspian region is far less investigated, though it is recently drawing ever-increasing attention by researchers owing to a multitude of climatic and environmental implications. This arid region is indeed an area of increasing desertification owing to climate change as well as to decades of disastrous environmental management, including the desiccation of the Aral Sea, with a loss of 90% of its original water volume in the last decades (Behzod et al., 2012; Breckle and Wucherer, 2012; Loodin, 2020; Sharma et al., 2018; Shen et al., 2016; Shi et al., 2014; Zhang et al., 2020).

The event of mineral dust incursion from Central Asia herein described occurred at the end of March 2020 and, to the best of our knowledge, has not been so far the object of an in-depth analysis though it was mentioned in a few papers devoted to other topics (Masic et al., 2020; Šikoparija, 2020) or described qualitatively in remote sensing or meteorological web pages (Mahovic et al., 2020; SNPA, 2020).

In this work, we present an in-depth analysis of this outstanding event based on the collection of high-resolution Optical Particle Counter number size distribution observed at three sites of NE Italy, i.e., at the two urban observatories in Bologna and Trieste, and the high altitude WMO-GAW Global observatory of Mt. Cimone (https://cimone.isac.cnr.it/). Data analysis includes an accurate meteorological assessment in order to identify the peculiar synoptic conditions leading to the event. Back-trajectories analysis was used to identify the source region. Aerosol behavior during transport over Italy was analyzed by Optical particle spectrometry, while multiple data based on remote sensing (satellites, LIDAR, and AERONET sun photometers) were employed to gain a dynamical 3D characterization of the mineral dust transport.

https://doi.org/10.5194/acp-2021-429
Preprint. Discussion started: 7 September 2021

Atmospheric Chemistry and Physics Discussions

After the Introduction section and a description of the measurement techniques, the discussion of the results is organized as follows: 1) In-depth synoptic analysis and directional analysis of the event; 2) Analysis of aerosol size distribution in Bologna, Trieste, and Mt. Cimone before, during and after the event; 3) Influence on aerosol mass load 4) Trend of AOD, aerosol vertical behavior and chemical composition of the dust event from satellite platforms. Finally, the main conclusions are summarized.

2 Materials and methods

2.1 Sampling sites

The Caspian dust event was highlighted during a long-term air-quality campaign by three Optical Particle Counters (see paragraph 2.3 for details) located in three different sampling sites.

Sampling in Bologna (BO) was carried out with one LOAC (Light Optical Aerosol Counter; MeteoModem, 77760 Ury, France) (Brattich et al., 2020b; Renard et al., 2016b, 2016c). The instrument was installed on the rooftop of the Department of Physics and Astronomy of the University of Bologna (44°29'58"N, 11°21'14"E, 62 m a.s.l.). Meteorological conditions (temperature, pressure, relative humidity, rain rate, wind speed and direction) in Bologna were also collected by a Davis Vantage Pro2 (Davis Instruments, Hayward, CA 94545, USA) on a 10-min time basis, close to LOAC.

In Trieste (TS), an OPC Multichannel Monitor (FAI Instruments S.r.l., Roma, Italy) (Dinoi et al., 2017) was placed in the air quality station of via Pitacco (45°37'29"N, 13°46'46"E, 30m a.s.l.), managed by the Regional Environmental Protection Agency (ARPA FVG - Agenzia Regionale per la Protezione dell'Ambiente del Friuli Venezia Giulia). Meteorological data for Trieste are available as open data on the ARPA FVG website (https://www.osmer.fvg.it/) on a 1-h time basis.

At the summit of Mt. Cimone (CMN, 44°11'37"N, 10°42'02"E, 2165 m a.s.l.), is located the only WMO-GAW global station in Italy and within the Mediterranean basin. The atmospheric measurements carried out at CMN can be considered representative for the baseline conditions of the Mediterranean basin free troposphere. An OPC (GRIMM 1.108) is continuously running since August 2002 to observe accumulation and coarse aerosol number size distribution. The OPC is placed on a TSP heated air inlet designed in the framework of EUSAAR project and following the ACTRIS recommendation for aerosol inlets.

For all sites, data analysis for the present work covers the period between 20 March and 5 April 2020, i.e. from a week before the beginning of the dust event (27 March) and until one week after the end of the event (31 March).

https://doi.org/10.5194/acp-2021-429
Preprint. Discussion started: 7 September 2021


Atmospheric Chemistry and Physics Discussions

2.2 Synoptic-scale conditions

The synoptic-scale main patterns related to the dust transport have been reconstructed and investigated based on the meteorological fields provided by the Global Forecast System (GFS) coupled model, produced by the National Centers for the Environmental Prediction (NCEP). In particular, we have analyzed the pressure field at the sea level (SLP) and the geopotential height at 500 (Z500) and 850 (Z850) hPa at 00:00 UTC for each day during the period of the event.

Besides, to locate and follow such long-range transport, we have used the regional air quality products of the Copernicus Atmosphere Monitoring Service (CAMS) (Marécal et al., 2015) in terms of particulate matter concentration (specifically PM_{10} fraction) at the height of 50 m above the surface. In detail, we have used the analysis output provided by the CAMS that merges model and observation data and ensures a high spatial resolution (~0.1 degrees) (CAMS, 2015).

Back-trajectories were also evaluated to confirm the origin of the studied mineral dust event from Central Asia. Back-trajectories are computed simulating the transport of air masses for a determined time frame until these reach a given "receptor" point at a specific time instant (Fleming et al., 2012; Rolph et al., 2017). In the specific case, 96-h back-trajectories were computed by Hybrid Single Particle Lagrangian Integrated Trajectory (HYSPLIT_4) model (Rolph et al., 2017; Stein et al., 2015) considering as receptor sites the three locations of the OPCs (see paragraph 2.3) over the whole period of the event. The computation was performed every six hours starting from 27 March 00:00 UTC until 31 March 18:00 UTC using GFS meteorological data at a 0.25-degree (27.8 km) resolution (National Centers for Environmental Prediction/National Weather Service/NOAA/US Department of Commerce, 2015). For each receptor site, trajectories were computed at three different heights to determine the impact of the arrival height on the trajectory analysis: 100, 1000, and 2000 m a.g.l. for Bologna (BO) and Trieste (TS), and 1700, 2200, 2700, and 3200 m a.g.l. for Mt. Cimone (CMN).

2.3 Optical Aerosol Counters (OPCs)

Optical particle counters (OPCs) are widely used for aerosol characterization (Brattich et al., 2015a, 2019, 2020b; Bulot et al., 2019; Kim et al., 2019). The advantages of this class of aerosol instrumentation over the traditional filter-based instruments are their portability, the relatively low cost, the availability of aerosol size distribution, and the possibility of acquiring PM data continuously and at high time resolution (down to 1 measurement s^{-1}) (Brattich et al., 2020b).

The three instruments employed in the sample sites (LOAC in BO, FAI in TS, and GRIMM at CMN, see paragraph 2.1), usually operated simultaneously for long-term data collection, are typically based on the principle of light scattering from aerosol particles, generally using a monochromatic high energy source such as a laser beam to detect and count particles. According to Mie scattering theory (Mie, 1908; Renard et al., 2016a), the intensity of scattered light is related to the particles' size, while the number of pulses of scattered

https://doi.org/10.5194/acp-2021-429
Preprint. Discussion started: 7 September 2021

Atmospheric Chemistry and Physics Discussions

light reaching the detector is related to the number of particles. This kind of instrument can retrieve a semi-continuous real-time analysis of the suspended particulate matter as a function of its diameter. In particular, the LOAC evaluates the scattering at two angles, 12° and 60°, the first being almost insensitive to the particles' refractive index, whereas the second is strongly sensitive to the refractive index (Renard et al., 2016b). GRIMM spectrometer detects aerosol particles from the scattered signal at 90°. All the OPC sensors operate at a 1 L min^{-1} air volume flow rate and with a scan frequency of 1 min. For the sake of homogeneity, all the data were averaged at 1-hour time resolution. All OPC data are reported as number concentration, in counts dm^{-3} (# L^{-1}).

Particle size distribution is obtained over 19 size bins for LOAC, 8 size bins for the FAI instrument, and 15 size bins for the GRIMM instrument, as reported in Table 1. A mean bin diameter was calculated for each size interval as previously indicated by Eq. 1 (Crilley et al., 2018):

$$D = LB\left[\frac{1}{4}\left(1+\left(\frac{UB}{LB}\right)^2\right)\left(1+\frac{UB}{LB}\right)\right]^{1/3} \quad (1)$$

where *LB* and *UB* are respectively the lower and the upper bin boundaries. While LOAC and GRIMM have well-defined minimum and maximum particle diameters for each bin, FAI OPC works in an integral mode: the count value of each bin was obtained by subtracting the value of the following one and for the computation of *D*, *LB* of the latter bin was set as *UB*.

Table 1. Size bins of the three OPCs. All reported values are in µm

	LOAC OPC		FAI OPC		GRIMM OPC	
Bin n°	**Boundaries**	**Mean diameter**	**Boundaries**	**Mean diameter**	**Boundaries**	**Mean diameter**
1	0.2 ÷ 0.3	0.253	> 0.28	0.343	0.3 ÷ 0.4	0.352
2	0.3 ÷ 0.4	0.352	> 0.4	0.452	0.4 ÷ 0.5	0.452
3	0.4 ÷ 0.5	0.452	> 0.5	0.606	0.5 ÷ 0.65	0.578
4	0.5 ÷ 0.6	0.551	> 0.7	0.915	0.65 ÷ 0.8	0.728
5	0.6 ÷ 0.7	0.651	> 1.1	1.59	0.8 ÷ 1.0	0.904
6	0.7 ÷ 0.9	0.804	> 2.0	2.53	1.0 ÷ 1.6	1.32
7	0.9 ÷ 1.1	1.00	> 3.0	4.08	1.6 ÷ 2.0	1.81
8	1.1 ÷ 3.0	2.19	> 5.0 ÷ 10.0	7.77	2.0 ÷ 3.0	2.53
9	3.0 ÷ 5.0	4.08			3.0 ÷ 4.0	3.52
10	5.0 ÷ 7.5	6.33			4.0 ÷ 5.0	4.52
11	7.5 ÷ 10.0	8.81			5.0 ÷ 7.5	6.33
12	10.0 ÷ 12.5	11.3			7.5 ÷ 10.0	8.81
13	12.5 ÷ 15.0	13.8			10.0 ÷ 15.0	12.7
14	15.0 ÷ 17.5	16.3			15.0 ÷ 20.0	17.6
15	17.5 ÷ 20.0	18.8			> 20.0	
16	20.0 ÷ 22.0	21.0				
17	22.0 ÷ 30.0	26.2				
18	30.0 ÷ 40.0	35.2				
19	40.0 ÷ 50.0	45.2				

https://doi.org/10.5194/acp-2021-429
Preprint. Discussion started: 7 September 2021

Atmospheric Chemistry and Physics Discussions

185 The LOAC aerosol range is between 0.20 and 50 µm, while the FAI working range is between 0.30 and 10 µm and the GRIMM working range lies between 0.3 and 20 µm.

Owing to the different ranges and number of bins of the used OPCs (Table 1), experimental data were homogenized as follows. Seven aerosol fractions were considered for comparison of the three OPC outputs, while two additional fractions were evaluated for LOAC only: "fr0.3", "fr0.4", "fr0.5", "fr0.7", "fr1.1", 190 "fr3", and "fr5" for all OPCs; "fr0.2" and "fr10" for LOAC only. Table 2 describes the processed fractions and the bin combination used for the comparison. Table 1 shows that also the GRIMM instrument could be used to evaluate "fr10". However, previous studies (Duchi et al., 2016; Marinoni et al., 2008; Sajani et al., 2012) highlighted that the presence of coarse particles is unusual on the top of CMN, except in cases of Saharan dust (Marinoni et al., 2008). Moreover, as described further on, the event herein analyzed, had 195 limited vertical development and did not affect significantly the top of Mt. Cimone as shown by the low counts of the coarser bins at this station. Therefore, we decided not to consider "fr10" for CMN.

Table 2. Fractions analyzed with LOAC, FAI OPC, and GRIMM, with the corresponding bin combinations (sums or differences)

Fraction	Size interval (µm)	LOAC	FAI	GRIMM
fr0.2	0.2 ÷ 0.3	bin1	--	--
fr0.3	0.3 ÷ 0.4	bin2	bin1 – bin2	bin1
fr0.4	0.4 ÷ 0.5	bin3	bin2 – bin3	bin2
fr0.5	0.5 ÷ 0.7	bin4 + bin5	bin3 – bin4	bin3
fr0.7	0.7 ÷ 1.1	bin6 + bin7	bin4 – bin5	bin4 + bin5
fr1.1	1.1 ÷ 3.0	bin8	bin5 – bin7	bin6 + bin7 + bin8
fr3	3.0 ÷ 5.0	bin9	bin7 – bin8	bin9 + bin10
fr5	5.0 ÷ 10.0	bin10 + bin11	bin8	bin11 + bin 12
fr10	> 10.0	Sum from bin11 to bin 19	--	--

200 Computations and graphs of time-series, particle size distributions, and number concentration to mass conversions were performed with R software (R Core Team, Vienna, Austria). Polar plots of the OPC fractions were calculated considering all data from 20 March to 6 April with the R package "*openair*" (Carslaw and Beevers, 2013; Carslaw and Ropkins, 2012).

2.4 Particulate matter concentrations and chemical speciation data

205 In addition to measurements from the OPCs, daily mean PM_{10} concentrations at two air quality stations of the ARPAE (Agenzia Prevenzione Ambiente Energia Emilia Romagna) Regional Environmental Protection Agency in Bologna (Porta San Felice and Giardini Margherita, respectively urban traffic and urban background station) were used. Data were obtained through the "*saqgetr"* R package (Grange, 2019).

https://doi.org/10.5194/acp-2021-429
Preprint. Discussion started: 7 September 2021

Atmospheric Chemistry and Physics Discussions

Furthermore, chemical speciation data (ions, carbonaceous fraction, and elements) sampled in Bologna and available as open data from ARPAE (https://www.arpae.it/it) were also analyzed to complement the other analyses.

2.5 AERONET (AErosol RObotic NETwork)

Aerosol optical depth (AOD) data retrieved from Aerosol Robotic Network (AERONET) ground-based remote sensing aerosol network at the site of Venice (Acqua Alta Oceanographic Tower - AAOT; 45°19'N, 12°30'E) were used as an independent method to confirm the dust aerosol transport event at the end of March 2020.

AERONET collaboration provides globally distributed observations of spectral aerosol optical depth (AOD), inversion products, and precipitable water in diverse aerosol regimes. For this work, version 3 AOD data and inversions computed for Level 2.0, i.e., quality assured (with pre- and post-field calibration applied, automatically cloud cleared, and manually inspected), were utilized. Total mode, fine mode, and coarse mode AOD at 500 nm were computed using a best-fit second-order polynomial. Finally, the AERONET inversion code provides aerosol optical properties in the total atmospheric column derived from the direct and diffuse radiation measured by AERONET Cimel sun/sky-radiometers (NASA, 2006). The output includes both retrieved aerosol parameters, which comprehends the volume size distribution, and parameters calculated based on the retrieved aerosol properties. The inversion algorithms are based on the following assumptions, i.e.: the atmosphere is considered as plane-parallel; the vertical distribution of aerosol is assumed homogeneous in the almucantar inversion and bi-layered for the principal plane inversion; aerosol particles are assumed to be partitioned in spherical and non-spherical components.

2.6 LIDAR Ceilometer

Aerosol vertical profiles collected in Milan (Diémoz et al., 2019; Ferrero et al., 2020) (45°31'N 9°12'E, 130 m asl, ~200 km northwest of Bologna) have been used to identify the signature of dust transport as well as to investigate its vertical extension and altitude. Such profiles were gathered by a Nimbus CHM15K system (Lufft, Germany) running within the Italian Automated Lidar Ceilometer network – Alice-net (www.alice-net.eu), coordinated by ISAC-CNR in partnership with other Italian research institutions and environmental agencies. It is a high-performance system providing vertical profiles of aerosols and clouds in the first 15 km of the atmosphere with a temporal resolution of 30 s and a vertical resolution of 15 m (Dionisi et al., 2018). Alice-net measurements have been and are usefully employed to detect altitude and temporal evolution of cloud layers (Ferrero et al., 2020) and to track transport of polluted (Diémoz et al., 2019) or mineral dust aerosol plumes (Gobbi et al., 2019) at different sites along the Italian peninsula.

https://doi.org/10.5194/acp-2021-429
Preprint. Discussion started: 7 September 2021

Atmospheric Chemistry and Physics Discussions

3 Results and discussion

3.1 Synoptic analysis

As documented later on, the likely source of the investigated episode of severe dust transport is the Central Asian southern desert region, arid but ecologically active, located between the eastern coast of the Caspian Sea and the steppes near the central Asia mountain ranges. Most of Turkmenistan and eastern Uzbekistan, as well as the Central Asian desert ecoregion to the North, can be considered a cold desert, in agreement with the inherent climatic class (BWk, according to the Köppen classification), with hot summers and cold winters, and annual precipitation of 125–170 mm year^{-1}, with winter and spring as the driest seasons. For these reasons, we have decided to analyze the pressure field at the sea level (SLP) and the geopotential height at 500 (Z500) and 850 (Z850) hPa in the period from 20 March to 30 March 2020. Figure 1 shows the geopotential maps (Z500) and the corresponding PM_{10} (50 m height) concentration maps derived from satellite observations for the most relevant days of the event, 25 – 28 March 2020.

On 20 March, at 500 hPa the geopotential height was high on the western Mediterranean basin and western Europe, due to a ridge expanded from Libya to Italy and Poland, while the pressure field at the sea level and the geopotential height at 850 hPa were uniform. On the Caspian deserts, the circulation was weak, even if, in the northern area, southern winds were flowing towards Uzbekistan and Kazakhstan. In the following three days, regarding Z500 the European anticyclone elongates versus northeast reaching Scandinavia on 23 March, and at the same time a trough developed from Russia extending to Bosnia and Albania; regarding SLP and Z850, an anticyclone developed on southern Sweden, activating a weak eastern flow directed from the southern Urals to Croatia. A southern flow established over the Caspian deserts, so designating the onset of the dust transport towards Europe and therefore Italy. On 24 March, at Z500 a narrow ridge was extending from the Azores to Baltic Republics, while a minimum formed between Caspian deserts and Italy; regarding SLP and Z850, a strong anticyclone was present over Lithuania and Belarus and a minimum north of the Caspian Sea were collaborating in originating both an intense eastern flow from the Caspian desert to the eastern Black Sea and another flow from the western Black Sea towards Italy. At that time, the Italian Adriatic regions were already affected by a strong NE flow, but still without dust, since the cloud on the evening of this day was just approaching the eastern Black Sea. On 25 March, at Z500 a cutoff was gradually filling over Italy, surrounded by a ridge from the UK to Belarus and another one west of Urals, in Asia. Regarding SLP, isobars in Fig 1a outline an almost linear corridor of flow between the Caspian deserts and Bosnia and Croatia, which veers North across the Bora door entering NE Italy, with a double curvature in correspondence of the Balkans; regarding Z850, the only remarkable flow is present between Romania and Croatia. At this stage, the dust cloud was crossing the Black Sea (Fig. 1b), still traveling near the surface. Important for the next evolution was also the minimum present in the SLP and at Z850 over Tunisia. On 26 March (Fig. 1c), the anticyclone extended towards the Black sea, joining with the one over Egypt, while the cutoff retreated to Italy and the western Mediterranean sea, promoting the shift of the SLP and Z850

https://doi.org/10.5194/acp-2021-429
Preprint. Discussion started: 7 September 2021


Atmospheric Chemistry and Physics Discussions

anticyclone to the north of the Black sea; the minimum over Tunisia shifted to Ionian sea, thus strengthening the flow along a corridor extended from the Caspian desert across the Black sea up to Romania and Bulgaria (Fig. 1d), and then from there to the Adriatic sea. Under these conditions, the most intense flow was observed. In the evening, the dust cloud reached Croatia. On 27 March (Fig. 1e), the trough at Z500 was located on the western Mediterranean basin, surrounded by anticyclones and ridges; SLP and Z850 cyclone moved over the Tyrrhenian sea, while the anticyclone expanded also over Romania; as a consequence, the main flow from the Caspian deserts, moving across the Black sea, headed towards Greece (Fig. 1f), veering toward NW thereafter affecting the Adriatic Sea and eastern Italy. The dust cloud touched down on the coast of the Adriatic regions (Friuli Venezia Giulia, Emilia Romagna, and Marche) in the evening. On 28 March (Fig. 1g), due to the weakening of the geopotential field at Z500 and Z850, as well as the SLP field, the flow from Romania to Italy weakened considerably. The circulation over NE Italy changed due to the influence of the anticyclonic curvature induced by a large high of SLP located between Iceland and Ireland, pivoting a strong surface northern flow from Scandinavia: a first impulse of cool easterly air mass shifted along the surface across the Po valley in the early morning, forming a shallow front (with few clouds) able to transport the dust cloud up to the border of Piedmont during the afternoon (Fig. 1h). In eastern Italy, instead, the local breeze circulation was prevailing. During the evening, a second easterly impulse crossed the Po Valley, this time accompanied by more clouds but without precipitations, and during the morning of 29 March reached also the northwestern Italian regions (Piedmont, Valle d'Aosta, and Liguria). At this time, approximately half of Italy was affected by the central Asian dust cloud, though over the NE sector the concentration had already decreased owing to a northerly air mass from the Alps. On this date, SLP and geopotential at Z850 and Z500 decreased abruptly in a corridor from Baltic republics to Greece, thus completely interrupting the easterly flow of dusty air. During the afternoon of the 29 March, the inflow of the arctic air mass moving across the Alps displaced southwards the mineral dust rich air mass over the Po Valley. Finally, on the 30 March, the cold front pushed by the Arctic airflow fully embraced the Po valley, thus definitely cleaning most of northern Italy.

https://doi.org/10.5194/acp-2021-429
Preprint. Discussion started: 7 September 2021

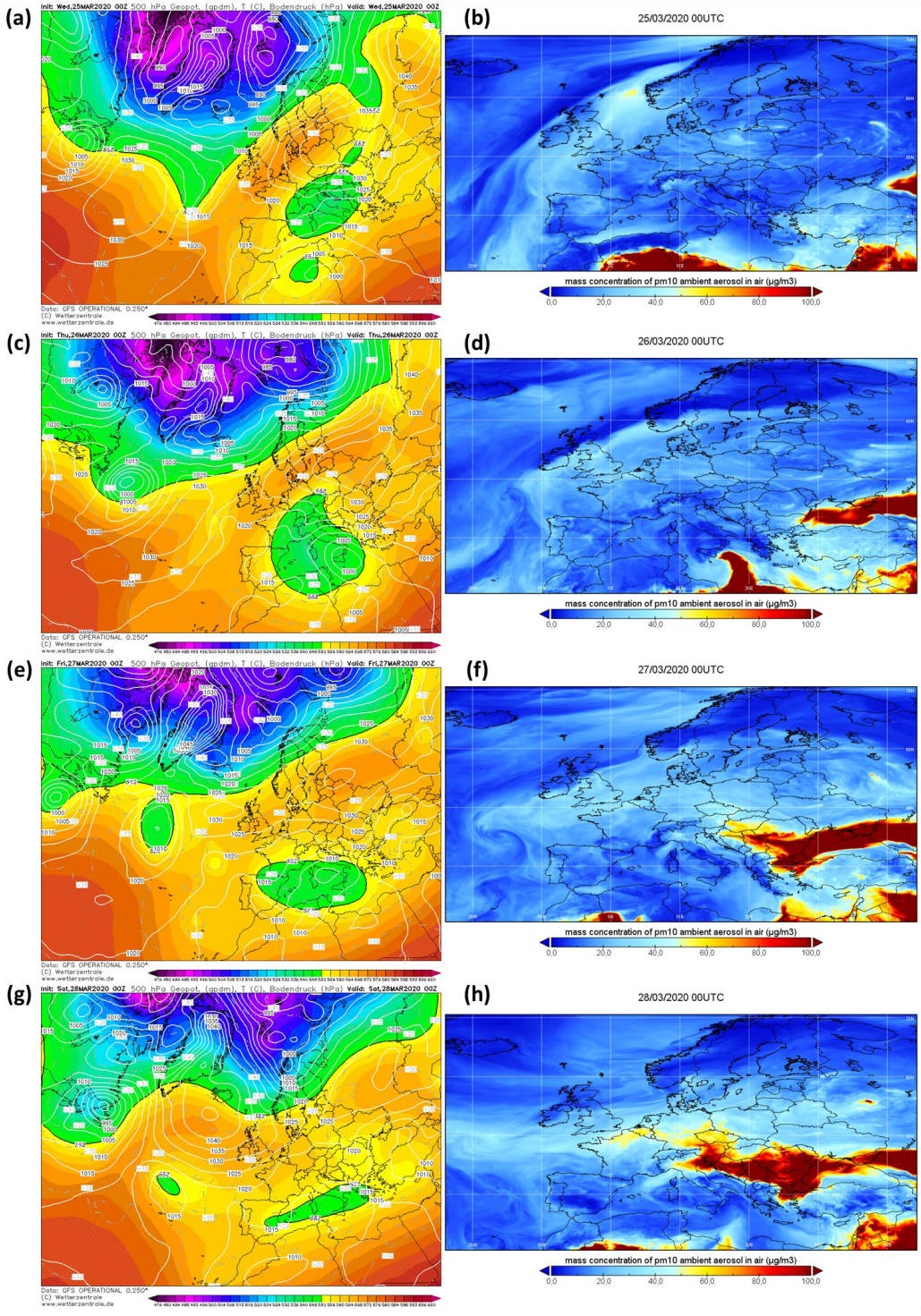

https://doi.org/10.5194/acp-2021-429
Preprint. Discussion started: 7 September 2021


Atmospheric Chemistry and Physics Discussions

Figure 1. Left part: analysis maps showing: 500 hPa geopotential height (colors, in dam) and temperature (dotted dashed grey lines, in °C) and surface pressure (white lines, in hPa) relative to the days a) 25 March; c) 26 March; e) 27 March; g) 28 March, chosen as the most significant synoptic maps for the episode studied. Source: Wetterzentrale.de (https://www.wetterzentrale.de/). Right part: PM_{10} concentration maps generated by Copernicus Atmosphere Monitoring Service (2020) at the height of 50 m above the surface, relative to the days b) 25 March; d) 26 March; f) 27 March; h) 28 March.

The easterly origin of the air mass originating the dust event over northern Italy was also confirmed by back-trajectory analyses. 96-h back-trajectories were computed using the three measurement sites (BO, TS, and CMN) as receptor points. The most relevant back-trajectories are reported in Figure 2 (for BO) and in the Appendix A for TS (Figure A1) and CMN (Figure A2).

Fig. 2a shows, in particular, the back-trajectory ending on 27 March 18:00 UTC in BO. Such date corresponds to the first peak due to the Caspian dust observed in TS by FAI-OPC, considered as the beginning of the event in Italy. Fig. 2a already indicates an airflow originating in the area between Caspian and Aral seas, with some intrusions from the Black and Mediterranean seas. The Caspian origin of air masses becomes even more evident in the following days (Fig. 2b and 2c). Then (Fig. 2d), on 30 March, a northern stream started to flow over northern Italy cleaning the air from the dust. The observation drawn from these back-trajectories confirms what was suggested by the synoptic analysis. The calculated trajectories, in the limits of the computational error, suggest that the Caspian dust, before arriving in Bologna, reached Trieste passing through the “Bora door” (a section of the Alps through which the Bora wind reaches Italy from the Balkan region).

This evidence is also confirmed by the computed back-trajectories for the TS measurement site shown in Figure A1. The ending times in Fig. A1 are the same as Fig. 2, and the conclusions that can be drawn are similar: an airflow originating in the Caspian region reached Trieste on 27 March (Fig A1a) and it continued in the following days (Fig. A1b and A1c) until a northern stream cleaned the air starting from 30 March (Fig. A1d).

Figure A2 shows, instead, some of the calculated back-trajectories for Mt. Cimone. In this case, an air mass with a possible north-African origin, with a strong component from the Aegean Sea, reached the site on 27 March (Fig. A2a), however, it did not give origin to visible peaks in the OPC time-series (Fig. 3c). Then, again (Fig. A2b and A2c), the peaks observed on 28 – 29 March can be associated with an airflow deriving from the Caspian region.

https://doi.org/10.5194/acp-2021-429
Preprint. Discussion started: 7 September 2021

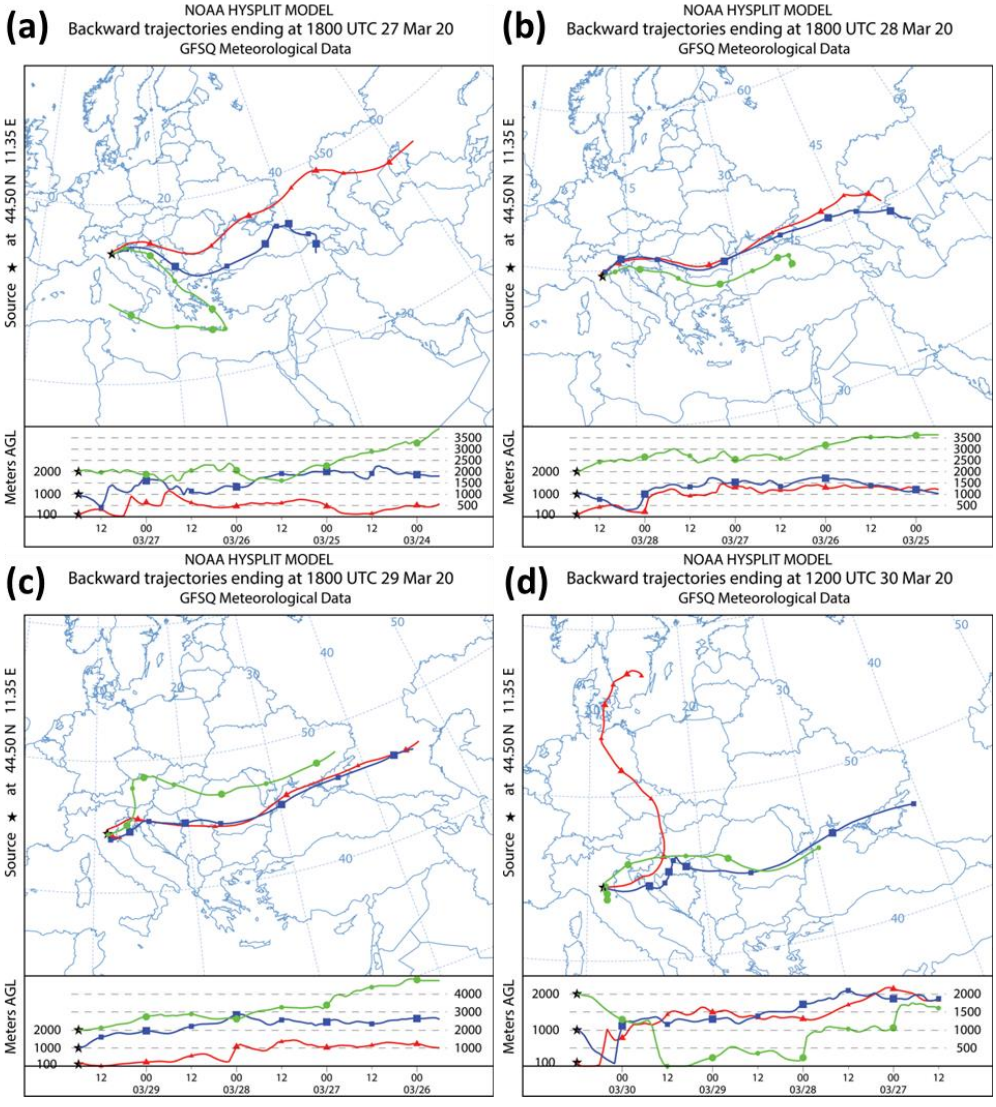

335 **Figure 2**. Back-trajectories (96-h backwards) ending at Bologna on a) 27 March 18:00 UTC; b) 28 March 18:00 UTC; c) 29 March 18:00 UTC; d) 30 March 12:00 UTC

3.2 Optical Aerosol Counters (OPCs)

3.2.1 Temporal trends and particle size distributions

The mineral dust outbreak produced a remarkable increase in particle number densities at all the three sites
340 investigated, i.e., Bologna, Trieste, and at the top of Mt. Cimone. This increase was remarkably high for the coarse fractions, a typical feature of mineral dust, in particular at both the urban stations.

https://doi.org/10.5194/acp-2021-429
Preprint. Discussion started: 7 September 2021

Atmospheric Chemistry and Physics Discussions

Figure 3 reports the temporal trend of the coarse fractions limited, for sake of simplicity, to fr5 (diameter 5-10 μm) for BO and TS, and the fraction fr3 (3-5 μm) for CMN. For the latter, fr3 was considered, instead of fr5, due to a large number of data below the detection limit for size bins > 7.5 microns, as previously reported in the Materials and methods section. This is consistent with a possible loss of larger particles due to gravitational settling during the transport at higher altitude. The complete OPC series are available in Appendix A (Fig. A3).

As reported in Figure 3, coarse particle number densities were very low both before and after the event, reflecting the typical size distribution at urban locations in the cold season, while the fairly low level in the fine fraction (Fig. A3) is likely due (besides the seasonal evolution pattern naturally leading to a decrease going towards the warmer season at this latitude) at least in part to the consequences of the lockdown imposed to stem the spread of the SARS-COV2 pandemic in Italy, from early March 2020 (Chauhan and Singh, 2020). The Asian dust plume impacted TS first, on 27 March during the afternoon, reaching BO (about 200 km east) the day after (please note the time lag of the order of one day at the two stations in Fig. 3a and 3b). Overall the event duration was of about three days, ceasing on 30 March in Trieste and on 31 March in Bologna. During this period, a general increase in suspended particle concentration, especially in the coarse fraction, was observed at all the stations in agreement with mineral dust properties and its resulting influence on PM mass load recorded at the time throughout several European stations (Mahovic et al., 2020). The dust plume reached CMN (Figure 3c) on 28 March, but the maximum concentrations were slightly lagged peaking between the afternoon of 29 March until 30 March. Another peak in CMN series is visible on 21 March, likely due to a genuine “high-pass” Saharan dust, which is not herein discussed being beyond the scope of the present work.

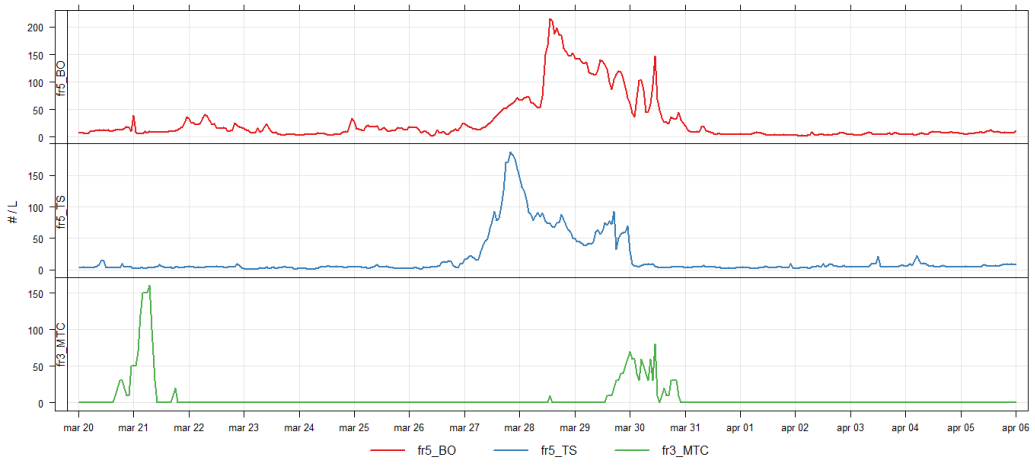

Figure 3. Temporal trends of fr5 (5.0 to 10.0 μm) at Bologna, red line, and Trieste, blue line, and of fr3 (3.0 to 5.0 μm) at Mt. Cimone, green line. Values are in Counts dm^{-3} (#/L)

https://doi.org/10.5194/acp-2021-429
Preprint. Discussion started: 7 September 2021


Atmospheric Chemistry and Physics Discussions

OPC data were associated with the meteorological parameters collected at the three sites, in particular, the connection with local wind speed and direction was evaluated using polar plots (Carslaw and Beevers, 2013). For the present study, we computed polar plots for fr5 of both cities and for fr3 of CMN as reported in Fig. 4. A conditional probability function (CPF) at the 90th percentile was used for computation in order to minimize pollution source effects and focus the computation only on the event of dust transport (Kurniawati et al., 2019). Polar plots of both cities (Fig. 4a and 4c) show a maximum CPF probability corresponding to the wind blowing from the east direction, in agreement with the advection of dust from the Caspian region to the study area. The wind speed corresponding to the two wind intensity maxima was about 3 m s^{-1} for Bologna and 7 m s^{-1} for Trieste. Fig. 4b and 4d report the wind intensity and direction pattern observed in the two cities during the study period. In particular, the plot highlights how the dust event was preceded and followed by weak winds, lower than 2 m s^{-1} and typical of the Po Valley basin, while during the event wind speed of about 15 up to 20 m s^{-1} was recorded in TS. The Easterly direction remains the most remarkable feature since this source area for air masses is fairly infrequent in Italy though acknowledged especially in the spring (Battison et al., 1988; Brattich et al., 2015b, 2020a; Dimitriou and Kassomenos, 2014).

https://doi.org/10.5194/acp-2021-429
Preprint. Discussion started: 7 September 2021

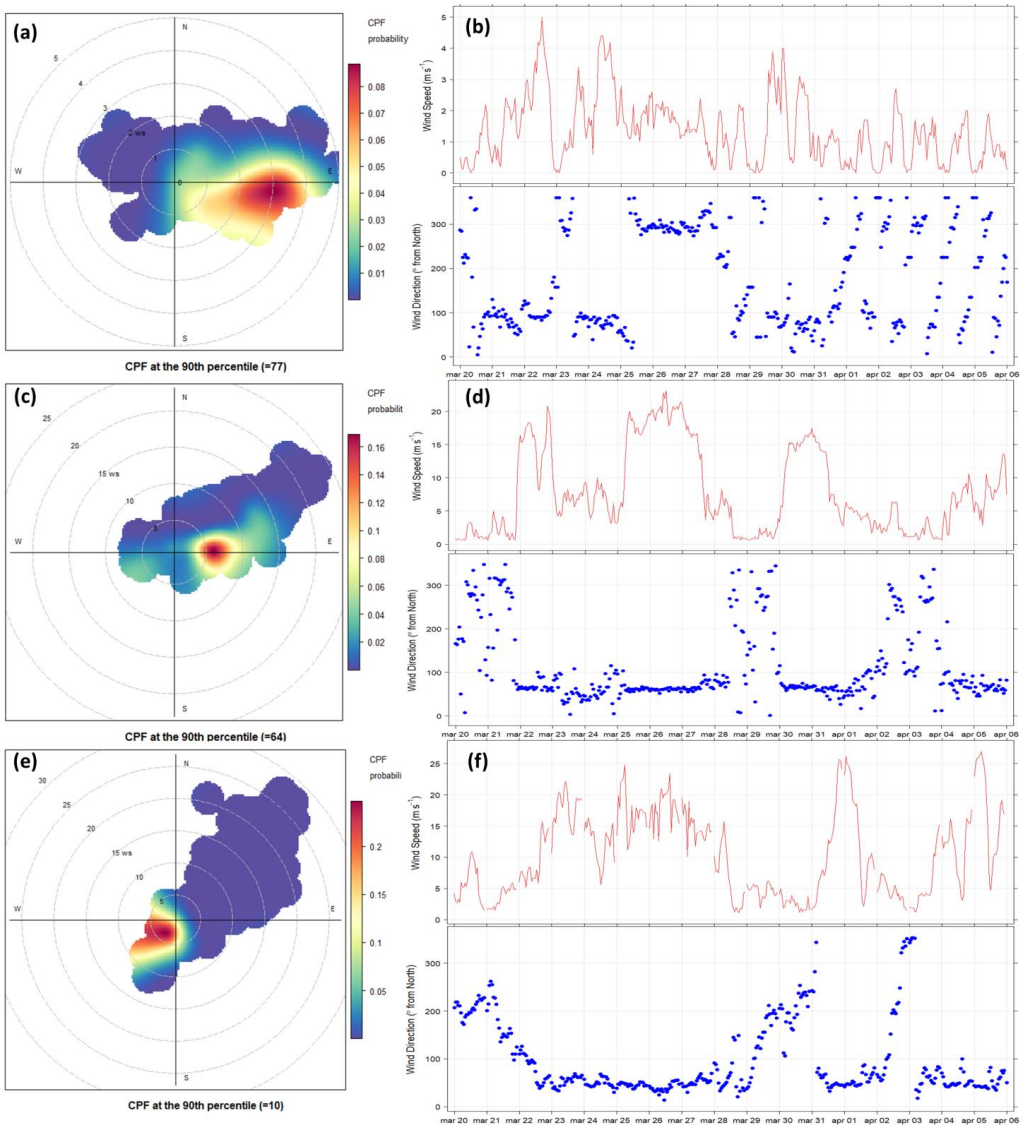

380

Figure 4. Right part: polar plots of a) fr5 for Bologna; c) fr5 for Trieste; e) fr3 for Mt. Cimone. Gray dashed circumferences indicate wind speed in m s^{-1}. Left part: wind speed (red line) and wind direction (blue points) from 20 March to 6 April 2020 for b) Bologna; d) Trieste; f) Mt. Cimone

385 The temporal behavior of particle number densities as a function of size is not the same (Fig. A3). At the three stations, mineral dust transport showed a stronger increase for the coarse fraction, while the increase in fine particles, although present, is generally slighter. Mt. Cimone, instead, showed an apparent strong increase in the fine fractions, but not in the coarse ones suggesting a depletion due to the influence of gravitational selection on particles with height.

https://doi.org/10.5194/acp-2021-429
Preprint. Discussion started: 7 September 2021

Atmospheric Chemistry and Physics Discussions

390 This information can be summarized by comparing particle size distributions at the three stations before, during, and after the event, as reported in Fig. 5. An overall increase in number densities is observed at all sites during the dust event. However, as reported in Fig. 5, the most significant deviations of the within-the-event period from both before- and after-event periods were observed starting from 0.7 µm in BO and TS, while at CMN also the finest particles undergo an increase during the event. This confirms the primary
395 influence of the dust on coarse particles, rather than on finer ones, at least in the two cities. This finding is different from Saharan dust outbreaks since, in this latter case, also the finest fractions increase, at least among the size range determined by OPC and/or from LIDAR observations (Brattich et al., 2015a; Denjean et al., 2016).

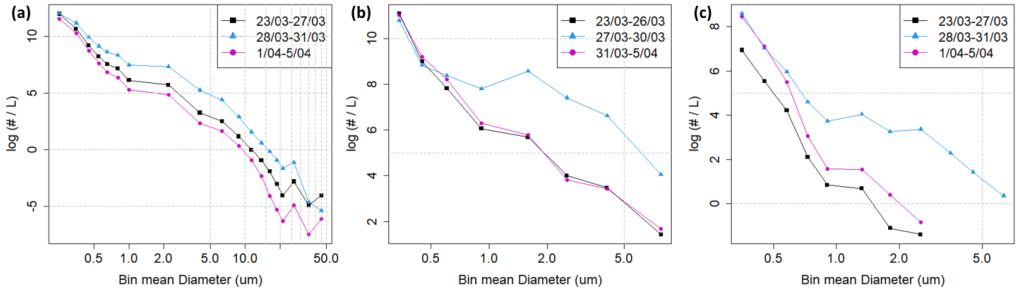

400 **Figure 5.** Particle size distributions for the OPCs: a) LOAC (Bologna); b) FAI (Trieste); c) GRIMM (Mt. Cimone). Abscissa values are in µm, ordinate values in log(# L^{-1}). Abscissa axis is on logarithmic scale

3.2.2 Particle Mass Concentrations

Number densities were eventually converted into daily PM_{10} mass loads using an algorithm based on an
405 average PM density of 1.65 g cm^{-3}, usually applied to urban aerosol composition, which may not accurately fit mineral dust aerosols with a different chemical composition (Brattich et al., 2020b; Gholamzade Ledari et al., 2020). Calculated daily PM_{10} mean in BO reached values of 79 and 74 µg m^{-3} respectively on 28 and 29 March (with an absolute maximum of 168 µg m^{-3} on 28 March 13:00 UTC), with a negative bias of about 12% with respect to the experimental values recorded by the Regional Environmental Protection Agency in
410 Bologna revealing an expected underestimate (Figure 6a). Calculated PM_{10} values are even higher at TS, where values of 107 and 124 µg m^{-3} were reached on 27 and 28 March (with maxima of 275 at 19:00 UTC and 246 µg m^{-3} at 23:00 UTC on 27 March). Recorded PM_{10} values in Bologna and Trieste are remarkably higher than the EU PM_{10} threshold (European Parliament, 2008) and 3-5 times the WHO recommendation (WHO for European, 2006) and the estimation of the desert dust load following the method suggested by
415 Barnaba et al. (2017) indicates values in the range of 66-108 µg m^{-3} at these two cities (Figure 6b).

In BO, PM_{10} was slightly above the EU threshold also on 30 March, (54 µg m^{-3}), while two relative maxima were detected on 27 March (36.4 µg m^{-3}) and 22 March (35.0 µg m^{-3}). The PM_{10} mean of the days before the

https://doi.org/10.5194/acp-2021-429
Preprint. Discussion started: 7 September 2021

Atmospheric Chemistry and Physics Discussions

event (excluding 22 March), which can be considered as representative of the typical background of the region likely due to the limited influence of vehicular emissions during the lockdown and the low influence of industrial activities in Bologna, were 15.0 μg m^{-3} 10.3 μg m^{-3} respectively prior and after the mineral dust outbreak event. A tail of the event was observed also in TS on 29 March with 79.4 μg m^{-3}. The PM_{10} daily mean value of the days before the event in TS was 11.4 μg m^{-3}, while that of the days immediately following the event was 13.9 μg m^{-3}.

An increase of calculated PM_{10} was observed also at Mt. Cimone with a maximum of 11 μg m^{-3} on 30 March 11:00 UTC. Although this value is very low compared to the ones of Bologna and Trieste, the increase is outstanding if compared with the mean PM_{10} values observed before and after the event: 0.11 and 0.35 μg m^{-3}, respectively in agreement with winter relative minima previously reported, due to the height (2173 m a.s.l.) and the cold-season decoupling of the mountain top from the PBL (Tositti et al., 2013).

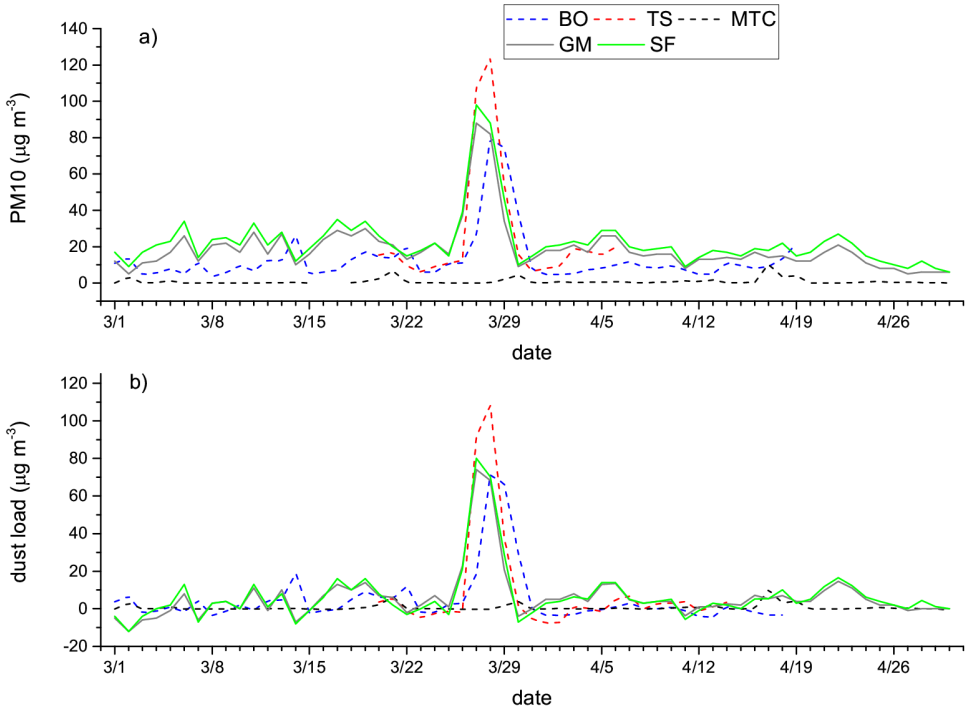

Figure 6. a) Daily mean PM_{10} values (a) and dust load (b) calculated over the March-April 2020 period. Dashed lines represent values calculated from the counts of the three optical particle counters in Bologna (BO), Trieste (TS), and Mt. Cimone (CMN), while solid lines represent concentration values recorded in Bologna at three air quality stations from the ARPAE network (Giardini Margherita GM, Porta San Felice SF).

https://doi.org/10.5194/acp-2021-429
Preprint. Discussion started: 7 September 2021

Atmospheric Chemistry and Physics Discussions

3.3 Ancillary analyses

3.3.1 AERONET (AErosol RObotic NETwork)

Figure 7 shows the Aerosol Optical Depth (AOD) data retrieved from AERONET ground-based remote sensing aerosol network at the site of Venice (Acqua Alta Oceanographic Tower - AAOT; 45°19'N, 12°30'E) around the period of the mineral dust outbreak event herein analyzed. Figure 7 shows very clearly the peculiar, steadily high aerosol optical depth value in the period 28 – 30 March and the simultaneously low value of the fine mode fraction, confirming the abrupt change in dust optical properties in agreement with the OPC data previously described.

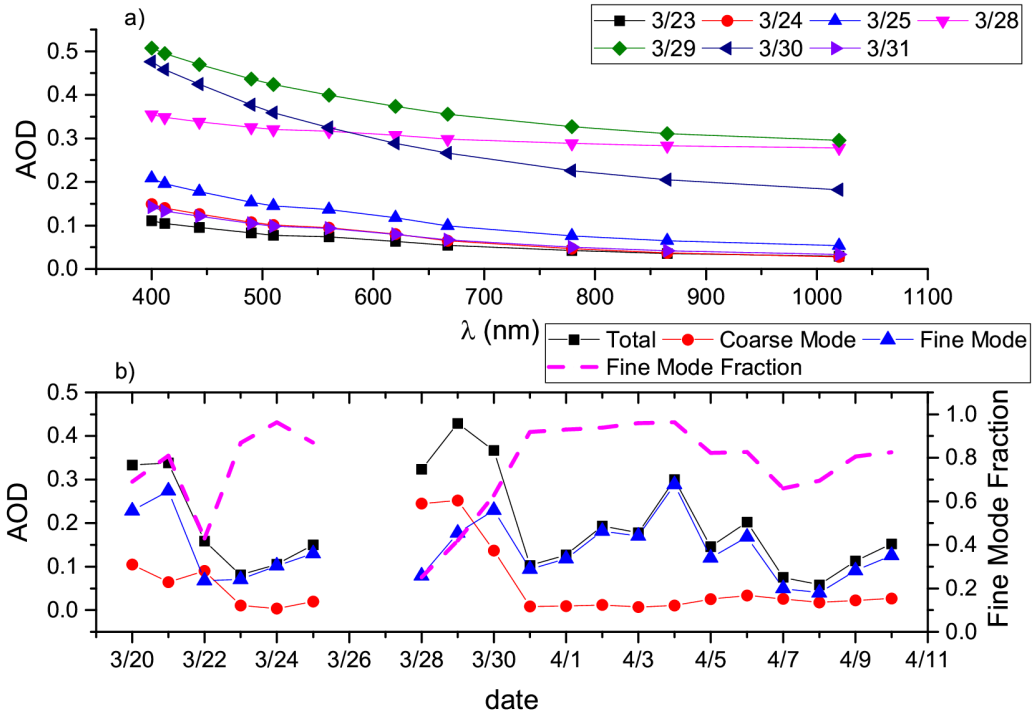

Figure 7. a) Aerosol Optical Depth (AOD) at different wavelengths and for different days of March 2020 detected at the AERONET site of Venice; b) time series of the total, coarse, and fine mode AOD, and fine mode fraction observed in March-April 2020 at the AERONET site of Venice.

https://doi.org/10.5194/acp-2021-429
Preprint. Discussion started: 7 September 2021


Atmospheric Chemistry and Physics Discussions

Even the volumetric size distributions retrieved by AERONET indicate the prominence of the coarse mode, i.e. of particles with an aerodynamic diameter > 1 μm, on 28 and 29 March in agreement with this observation and with the particle size distributions from OPC readings in BO and TS (Fig. A4).

3.3.2 LIDAR Ceilometer

Images from a LIDAR ceilometer from Alice-net (Dionisi et al., 2018) located in Milan were employed to derive information on aerosol vertical distribution and of the dynamics of the atmospheric lowest layers. The sensor achieves excellent signal quality thanks to its stable wavelength and its Nd:YAG narrow-beam microchip laser operating in the 1064 nm range. In addition, its technology enables efficient daylight suppression and reduces temperature fluctuations to a minimum. Figure 8 shows the vertical profiles observed during the event, showing an approximate thickness of about 2 km above ground level. This observation indicates another peculiarity of this mineral dust event, which, differently from Saharan dust plumes typically reaching and shifting aloft between 1500 and 4000 m a.s.l. (Jorba et al., 2004; Soupiona et al., 2020), traveled at relatively low atmospheric altitude, reasonably due to the low temperatures at the source and to the reduced convective activity resulting from the higher latitude and season as compared to the Sahara desert. The relatively low travel height of the dust plume caused the gravitational settling of the heaviest particles in the proximity of the ground, in agreement with the size distribution data observed at Mt. Cimone as shown in Figure A3c.

Figure 8 shows also that the yellow layer was somewhat deeper during the first three hours of 28 March than during the rest of the day; this observation likely indicates that early in the morning the dust plume was capped by a cloud top, reasonably caused by the irruption of the easterly cold front towards the Po Valley. The layer was shallower from 4:00 UTC on. Signals of convective activity appeared between 10:00 - 15:00 UTC, as indicated by the more intense orange vertical swipes linked to the rising thermals. In the evening, the layer was even shallower, due to the nocturnal cooling suppressing vertical motions. In general, the thinning of the mixing layer during dust transports, confirmed also by the analysis of the radiosoundings of the period, is linked to the high concentrations of aerosols in the troposphere which reduce the amount of solar radiation reaching the ground, in turn reducing sensible heat fluxes that drive the diurnal evolution of temperature and the PBL (Li et al., 2017; Pandolfi et al., 2014; Salvador et al., 2019). From 20:00 UTC on, 2 km high clouds appeared, probably linked to the arrival of the cold front from N-NE, while the yellow layer rose again because of wind-induced turbulence. The following day, thermals appeared again between 8:00 and 15:00 UTC, while the signal of Arctic air masses can be observed from 20:00 UTC on.

https://doi.org/10.5194/acp-2021-429
Preprint. Discussion started: 7 September 2021

Atmospheric Chemistry and Physics Discussions

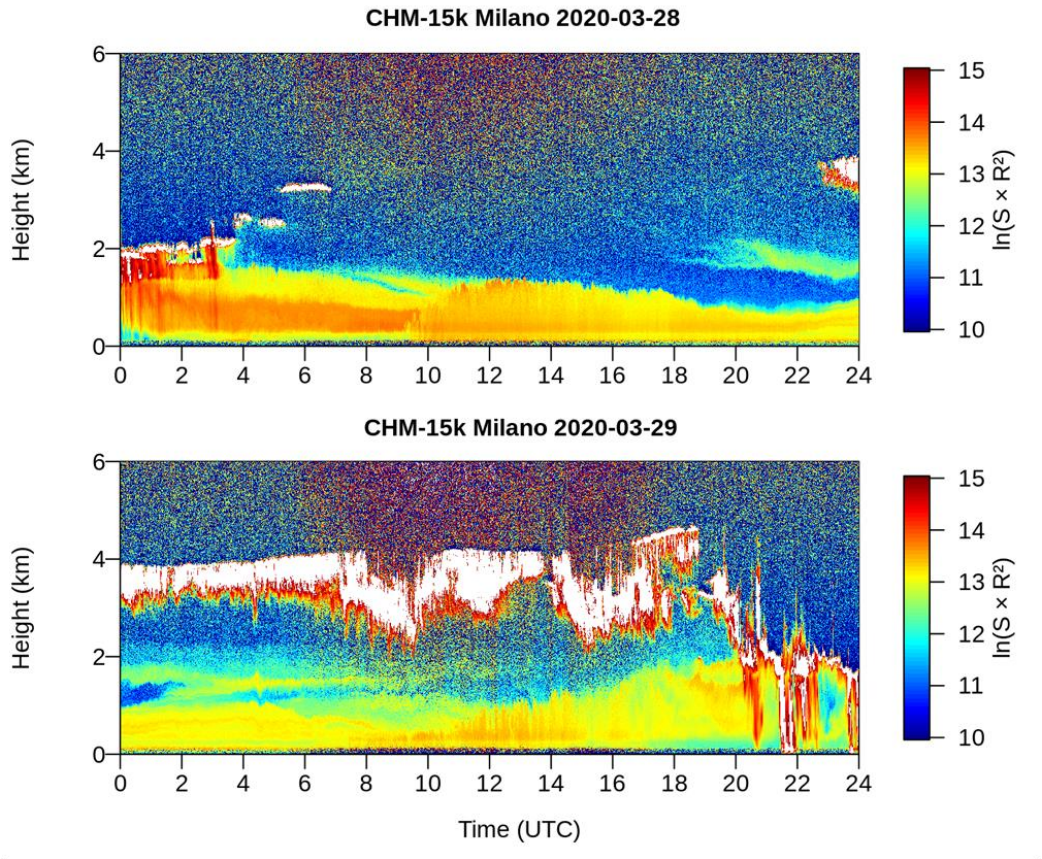

Figure 8. Vertical profiling from the automated LIDAR ceilometer located in Milan on 28 and 29 March 2020.

3.3.3 Chemical composition

The change in dust optical properties is in agreement with the concurrent change in aerosol composition at the Bologna Gobetti ARPAE station (Figure 9). Indeed, the arrival of the dust plume from the Aralkum desert was connected with an increase in some major particulate components (i.e., nitrate, sulfate, elemental carbon) and trace elements (K, Pb) likely in association with the entrainment of air pollution when the air mass passed over the Balkans (Evangeliou et al., 2021) as well as of some trace elements (Na, Ca, Mg, Fe), some of which typically crustal (Ca and Mg, Fe) due to the mineral dust matrix or marine (Na), most likely from the Adriatic Sea. The entrainment of anthropogenic pollution and marine aerosols together with the crustal material originated from the Aralkum might have been favored by the low boundary layer previously observed, an aspect which has been put in connection with the exacerbation of the toxicological properties of dust aerosols (Pandolfi et al., 2014).

https://doi.org/10.5194/acp-2021-429
Preprint. Discussion started: 7 September 2021

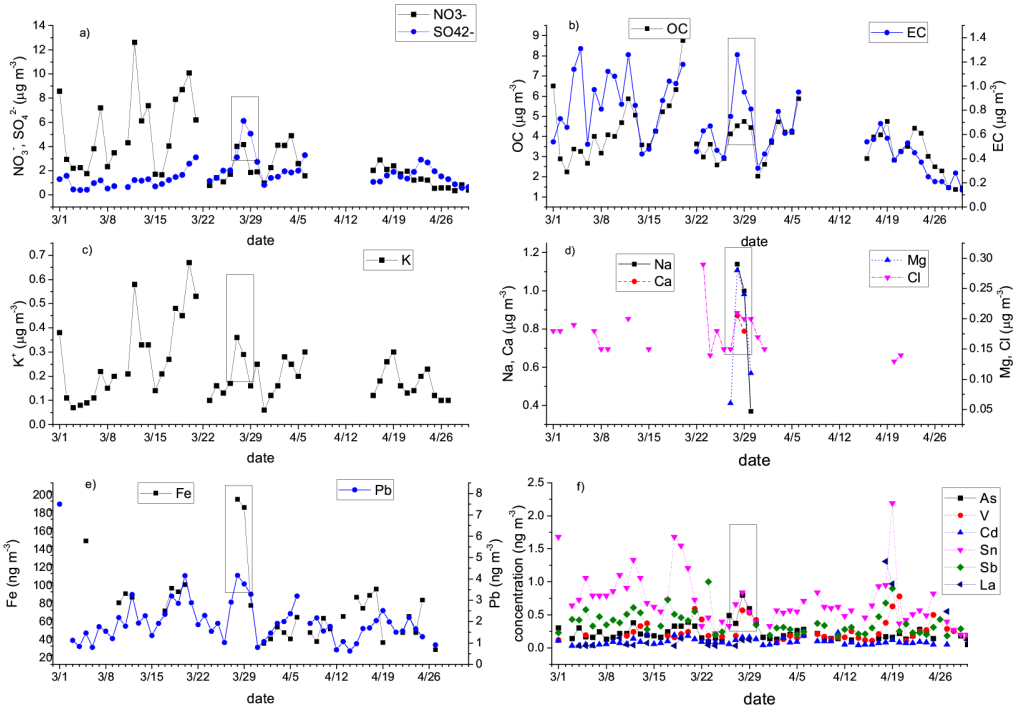

495 **Figure 9.** Concentration of major components and trace elements analyzed in $PM_{2.5}$ particulate samples at the Bologna Gobetti ARPAE air quality station during March-April 2020 period: a) nitrate NO_3^- and sulfate SO_4^{2-}; b) carbonaceous components organic and elemental carbon (OC and EC); c) potassium ion (K^+); d) Na, Ca, Mg and Cl; e) Fe and Pb; f) As, V, Cd, Sn, Sb, and La. The boxes enclose the dates of the dust incursion over Northern Italy.

500

https://doi.org/10.5194/acp-2021-429
Preprint. Discussion started: 7 September 2021

Atmospheric Chemistry and Physics Discussions

4 Conclusions

This work presents a detailed investigation of a mineral dust event that reached northern Italy at the end of March 2020. The peculiarity of this event is mainly associated with its origin, which can be traced back to the desert region surrounding the Caspian Sea, in central Asia. Its origin was confirmed by the concurrent analysis of the synoptic configuration together with satellite data of AOD and the calculation of back-trajectories for the study period. In particular, while it is well known how Southern Europe is often subjected to mineral dust incursions from the Sahara desert, transport of mineral dust originated in the Caspian area impacts frequently eastern Asia rather than Europe.

Data collected from three optical particle counters (OPCs), located at two different cities, Bologna and Trieste, and at one high-altitude i.e. the WMO-GAW Mt. Cimone station, all in northern Italy, was used to study the event at high time resolution. The use of OPCs allowed characterizing accurately the size distribution of this anomalous mineral dust event, to understand its features over time.

The results demonstrated that the transport of mineral dust affected mostly the concentration of coarse fraction at all three sites, in particular those with a mean diameter higher than 0.7 μm. The fine fraction appeared negligibly affected by the central Asian mineral dust outburst, its concentration being similar to that observed before and after the event. Anyhow, the coarse fraction was affected by the event to the point that PM_{10} concentration in Bologna exceeded up to twice - three times the WHO limit, in a period in which anthropogenic emissions were strongly reduced by the lockdown imposed in Italy to contrast the spread of the SARS-COV2 virus.

Overall, these results demonstrate how the concurrent analysis of multiple meteorological information and atmospheric composition data is needed to deepen our understanding of the variety of physicochemical processes connected with aerosols and their interactions. These results can be extremely important for their potential climatological implications owing to the projected increases in the frequency of dust storms resulting from the combined effects of increasing temperatures, increasing drought, and soil erosion.

https://doi.org/10.5194/acp-2021-429
Preprint. Discussion started: 7 September 2021

Atmospheric Chemistry and Physics Discussions

Data availability

OPC observations and HYSPLIT back-trajectories used for this investigation are available upon request to the corresponding author (laura.tositti@unibo.it).

Synoptic maps are available on the wetterzentrale web archive: https://www.wetterzentrale.de/.

CAMS data are freely available on the Copernicus website at: https://ads.atmosphere.copernicus.eu/ or https://atmosphere.copernicus.eu/.

NASA AERONET observations are available at: https://aeronet.gsfc.nasa.gov/.

The lidar ceilometer images from the Alice-net automated images from Milan are available by contacting the PI Luca Di Liberto (l.diliberto@isac.cnr.it).

Aerosol chemical speciation data are available on the ARPAE open data portal at: https://dati.arpae.it/.

Author contributions

LT, EB, and FP designed the study. CC led the synoptic analysis. PM led calculation and analysis of HYSPLIT back-trajectories. AZ, EB, and AB developed the analysis methodology and led the analysis of observational data with contributions from all coauthors. AM provided and analyzed data for the Mt. Cimone station. LT, EB, and AZ wrote the manuscript with contributions from all coauthors.

Competing interests

The authors declare that they have no conflict of interest.

Acknowledgments

We gratefully acknowledge Dr. Marco Bellini and Dr. Fulvio Stel from ARPA FVG Regional Environmental Protection Agency for providing data at the Trieste via Pitacco and via del Ponticello stations. Open data of PM chemical speciation at the Bologna via Gobetti sampling site were provided ARPAE Regional Environmental Protection Agency. The HYSPLIT transport and dispersion model and/or READY website (https://www.ready.noaa.gov) used in this publication were provided by the NOAA Air Resources Laboratory (ARL). We wish to thank the NASA-GSFC AERONET team, and the PI Giuseppe Zibordi and his staff for establishing and maintaining the AAOT Venice site used in this investigation. We also thank the Alice-net automated LIDAR ceilometer network and the PI Luca Di Liberto from ISAC-CNR Rome for providing access to the LIDAR ceilometer images from Milan.

Financial support

https://doi.org/10.5194/acp-2021-429
Preprint. Discussion started: 7 September 2021

This paper is published with the contribution of the Department of Excellence program financed by the Ministry of Education, University and Research (MIUR, L. 232 del 01/12/2016).

The study was also supported by a Research Grant from CARISBO Foundation, Bologna, Italy.

Monte Cimone station has received funding from the European Union's Horizon 2020 Research and Innovation Programme under grant agreement No 654109.

https://doi.org/10.5194/acp-2021-429
Preprint. Discussion started: 7 September 2021

References

Adebiyi, A. A. and Kok, J. F.: Climate models miss most of the coarse dust in the atmosphere, Sci. Adv., 6(15), doi:10.1126/sciadv.aaz9507, 2020.

Bangert, M., Nenes, A., Vogel, B., Vogel, H., Barahona, D., Karydis, V. A., Kumar, P., Kottmeier, C. and Blahak, U.: Saharan dust event impacts on cloud formation and radiation over Western Europe, Atmos. Chem. Phys., 12(9), 4045–4063, doi:10.5194/acp-12-4045-2012, 2012.

Barkan, J. and Alpert, P.: Synoptic analysis of a rare event of Saharan dust reaching the Arctic region, Weather, 65(8), 208–211, doi:10.1002/wea.503, 2010.

Barnaba, F., Bolignano, A., Di Liberto, L., Morelli, M., Lucarelli, F., Nava, S., Perrino, C., Canepari, S., Basart, S., Costabile, F., Dionisi, D., Ciampichetti, S., Sozzi, R. and Gobbi, G. P.: Desert dust contribution to PM10 loads in Italy: Methods and recommendations addressing the relevant European Commission Guidelines in support to the Air Quality Directive 2008/50, Atmos. Environ., 161, 288–305, doi:10.1016/j.atmosenv.2017.04.038, 2017.

Battison, G. A., Degetto, S., Gerbasi, R., Sbrignadello, G. and Tositti, L.: Fallout distribution in Padua and Northeast Italy after the chernobyl nuclear reactor accident, J. Environ. Radioact., 8(2), 183–191, doi:10.1016/0265-931X(88)90025-2, 1988.

Behzod, G., Su-Chin, C. and Dilmurod, G.: Changes in water volume of the Aral Sea after 1960, Appl. Water Sci., 2, 285–291, doi:https://doi.org/10.1007/s13201-012-0048-z, 2012.

Belosi, F., Conte, M., Gianelle, V., Santachiara, G. and Contini, D.: On the concentration of SARS-CoV-2 in outdoor air and the interaction with pre-existing atmospheric particles, Environ. Res., 193, doi:10.1016/j.envres.2020.110603, 2021.

Brattich, E., Riccio, A., Tositti, L., Cristofanelli, P. and Bonasoni, P.: An outstanding Saharan dust event at Mt. Cimone (2165 m a.s.l., Italy) in March 2004, Atmos. Environ., 113, 223–235, doi:10.1016/j.atmosenv.2015.05.017, 2015a.

Brattich, E., Hernández-Ceballos, M. A., Cinelli, G. and Tositti, L.: Analysis of 210Pb peak values at Mt. Cimone (1998-2011), Atmos. Environ., 112, 136–147, doi:10.1016/j.atmosenv.2015.04.020, 2015b.

Brattich, E., Serrano Castillo, E., Guilietti, F., Renard, J.-B., Tripathi, S. N., Ghosh, K., Berthet, G., Vignelles, D. and Tositti, L.: Measurements of aerosols and charged particles on the BEXUS18 stratospheric balloon, Ann. Geophys., 37, 389–403, doi:10.5194/angeo-37-389-2019, 2019.

Brattich, E., Orza, J. A. G., Cristofanelli, P., Bonasoni, P., Marinoni, A. and Tositti, L.: Advection pathways at the Mt. Cimone WMO-GAW station: Seasonality, trends, and influence on atmospheric composition,

Atmos. Environ., 234, doi:10.1016/j.atmosenv.2020.117513, 2020a.

Brattich, E., Bracci, A., Zappi, A., Morozzi, P., Sabatino, S. Di, Porcù, F., Nicola, F. Di and Tositti, L.: How to get the best from low-cost particulate matter sensors: Guidelines and practical recommendations, Sensors (Switzerland), 20(11), 1–33, doi:10.3390/s20113073, 2020b.

Breckle, S.-W. and Wucherer, W.: The Aralkum, a Man-Made Desert on the Desiccated Floor of the Aral Sea (Central Asia), edited by L. A. Dimeyeva and N. P. Ogar, Springer., 2012.

Bulot, F. M. J., Johnston, S. J., Basford, P. J., Easton, N. H. C., Apetroaie-Cristea, M., Foster, G. L., Morris, A. K. R., Cox, S. J. and Loxham, M.: Long-term field comparison of multiple low-cost particulate matter sensors in an outdoor urban environment, Sci. Rep., 9(1), doi:10.1038/s41598-019-43716-3, 2019.

Calidonna, C. R., Avolio, E., Gullì, D., Ammoscato, I., De Pino, M., Donateo, A. and Feudo, T. Lo: Five years of dust episodes at the Southern Italy GAW regional coastal mediterranean observatory: Multisensors and modeling analysis, Atmosphere (Basel)., 11(5), doi:10.3390/ATMOS11050456, 2020.

CAMS: CAMS documentation Webpage, [online] Available from: https://confluence.ecmwf.int/display/CKB/CAMS+Regional%3A+European+air+quality+analysis+and+forecast+data+documentation (Accessed 10 May 2021), 2015.

Carslaw, D. C. and Beevers, S. D.: Characterising and understanding emission sources using bivariate polar plots and k-means clustering, Environ. Model. Softw., 40, 325–329, doi:10.1016/j.envsoft.2012.09.005, 2013.

Carslaw, D. C. and Ropkins, K.: Openair - An r package for air quality data analysis, Environ. Model. Softw., 27–28, 52–61, doi:10.1016/j.envsoft.2011.09.008, 2012.

Chauhan, A. and Singh, R. P.: Decline in PM2.5 concentrations over major cities around the world associated with COVID-19, Environ. Res., 187, doi:10.1016/j.envres.2020.109634, 2020.

Crilley, L. R. ., Shaw, M. ., Pound, R. ., Kramer, L. J. ., Price, R. ., Young, S. ., Lewis, A. C. . and Pope, F. D.: Evaluation of a low-cost optical particle counter (Alphasense OPC-N2) for ambient air monitoring, Atmos. Meas. Tech., 11, 709–720, doi:10.5194/amt-11-709-2018, 2018.

Denjean, C., Cassola, F., Mazzino, A., Triquet, S., Chevaillier, S., Grand, N., Bourrianne, T., Momboisse, G., Sellegri, K., Schwarzenbock, A., Freney, E., Mallet, M. and Formenti, P.: Size distribution and optical properties of mineral dust aerosols transported in the western Mediterranean, Atmos. Chem. Phys., 16(2), 1081–1104, doi:10.5194/acp-16-1081-2016, 2016.

Diémoz, H., Barnaba, F., Magri, T., Pession, G., Dionisi, D., Pittavino, S., Tombolato, I. K. F., Campanelli, M., Ceca, L. S. Della, Hervo, M., Di Liberto, L., Ferrero, L. and Gobbi, G. P.: Transport of Po Valley aerosol

https://doi.org/10.5194/acp-2021-429
Preprint. Discussion started: 7 September 2021


Atmospheric Chemistry and Physics Discussions

pollution to the northwestern Alps-Part 1: Phenomenology, Atmos. Chem. Phys., 19(5), 3065–3095, doi:10.5194/acp-19-3065-2019, 2019.

Dimitriou, K. and Kassomenos, P.: Indicators reflecting local and transboundary sources of PM2.5 and PMCOARSE in Rome - impacts in air quality, Atmos. Environ., 96, 154–162, doi:10.1016/j.atmosenv.2014.07.029, 2014.

Dinoi, A., Donateo, A., Conte, M., Conte, M. and Belosi, F.: Comparison of atmospheric particle concentration measurements using different optical detectors: Potentiality and limits for air quality applications, Meas. J. Int. Meas. Confed., 106, 274–282, doi:10.1016/j.measurement.2016.02.019, 2017.

Dionisi, D., Barnaba, F., Diémoz, H., Di Liberto, L. and Gobbi, G. P.: A multiwavelength numerical model in support of quantitative retrievals of aerosol properties from automated lidar ceilometers and test applications for AOT and PM10 estimation, Atmos. Meas. Tech., 11(11), 6013–6042, doi:10.5194/amt-11-6013-2018, 2018.

Domínguez-Rodríguez, A., Báez-Ferrer, N., Abreu-González, P., Rodríguez, S., Díaz, R., Avanzas, P. and Hernández-Vaquero, D.: Impact of Desert Dust Events on the Cardiovascular Disease: A Systematic Review and Meta-Analysis, J. Clin. Med., 10(4), 727, doi:10.3390/jcm10040727, 2021.

Duchi, R., Cristofanelli, P., Landi, T. C., Arduini, J., Bonafe, U., Bourcier, L., Busetto, M., Calzolari, F., Marinoni, A., Putero, D. and Bonasoni, P.: Long-term (2002-2012) investigation of Saharan dust transport events at Mt. Cimone GAW global station, Italy (2165 m a.s.l.), Elementa, 2016, doi:10.12952/journal.elementa.000085, 2016.

European Parliament: Directive 2008/50/EC of the European Parliament and of the Council of 21 May 2008 on Ambient Air Quality and Cleaner Air for Europe, European Commission, Brussels, Belgium. [online] Available from: http://eur-lex.europa.eu/legal-content/EN/TXT/PDF/?uri=CELEX:32008L0050&from=EN, 2008.

Evangeliou, N., Platt, S. M., Eckhardt, S., Lund Myhre, C., Laj, P., Alados-Arboledas, L., Backman, J., Brem, B. T., Fiebig, M., Flentje, H., Marinoni, A., Pandolfi, M., Yus-Dìez, J., Prats, N., Putaud, J. P., Sellegri, K., Sorribas, M., Eleftheriadis, K., Vratolis, S., Wiedensohler, A. and Stohl, A.: Changes in black carbon emissions over Europe due to COVID-19 lockdowns, Atmos. Chem. Phys., 21(4), 2675–2692, doi:10.5194/acp-21-2675-2021, 2021.

Ferrero, L., Gregorič, A., Močnik, G., Rigler, M., Cogliati, S., Barnaba, F., Di Liberto, L., Gobbi, G. P., Losi, N. and Bolzacchini, E.: The impact of cloudiness and cloud type on the atmospheric heating rate of black and brown carbon, Atmos. Chem. Phys., 1–33, doi:10.5194/acp-2020-264, 2020.

Fleming, Z. L., Monks, P. S. and Manning, A. J.: Review: Untangling the influence of air-mass history in

interpreting observed atmospheric composition, Atmos. Res., 104–105, 1–39, doi:10.1016/j.atmosres.2011.09.009, 2012.

Fubini, B. and Fenoglio, I.: Toxic potential of mineral dusts, Elements, 3(6), 407–414, doi:10.2113/GSELEMENTS.3.6.407, 2007.

García-Pando, C. P., Stanton, M. C., Diggle, P. J., Trzaska, S., Miller, R. L., Perlwitz, J. P., Baldasano, J. M., Cuevas, E., Ceccato, P., Yaka, P. and Thomson, M. C.: Soil dust aerosols and wind as predictors of seasonal meningitis incidence in niger, Environ. Health Perspect., 122(7), 679–686, doi:10.1289/ehp.1306640, 2014.

Gholamzade Ledari, D., Hamidi, M. and Shao, Y.: Evaluation of the 13 April 2011 frontal dust storm in west Asia, Aeolian Res., 44, doi:10.1016/j.aeolia.2020.100592, 2020.

Gobbi, G. P., Barnaba, F., Di Liberto, L., Bolignano, A., Lucarelli, F., Nava, S., Perrino, C., Pietrodangelo, A., Basart, S., Costabile, F., Dionisi, D., Rizza, U., Canepari, S., Sozzi, R., Morelli, M., Manigrasso, M., Drewnick, F., Struckmeier, C., Poenitz, K. and Wille, H.: An inclusive view of Saharan dust advections to Italy and the Central Mediterranean, Atmos. Environ., 201, 242–256, doi:10.1016/j.atmosenv.2019.01.002, 2019.

Grange, S. K.: Technical note: saqgetr R package (Version 0.1). [online] Available from: https://drive.google.com/file/d/1IgDODHqBHewCTKLdAAxRyR7ml8ht6Ods/view, 2019.

IPCC Working Group I: WORKING GROUP I CONTRIBUTION TO THE IPCC FIFTH ASSESSMENT REPORT CLIMATE CHANGE 2013 : THE PHYSICAL SCIENCE BASIS, Final Draft Underlying Scientific-Technical Assessment, Ipcc, (January 2014), 103, doi:10.1017/CBO9781107415324, 2013.

Jorba, O., Pérez, C., Rocadenbosch, F. and Baldasano, J. M.: Cluster analysis of 4-day back trajectories arriving in the Barcelona area, Spain, from 1997 to 2002, J. Appl. Meteorol., 43(6), 887–901, doi:10.1175/1520-0450(2004)043<0887:CAODBT>2.0.CO;2, 2004.

Kaskaoutis, D. G., Houssos, E. E., Minvielle, F., Rashki, A., Chiapello, I., Dumka, U. C. and Legrand, M.: Long-term variability and trends in the Caspian Sea – Hindu Kush Index: Influence on atmospheric circulation patterns, temperature and rainfall over the Middle East and Southwest Asia, Glob. Planet. Change, 169, 16–33, doi:10.1016/j.gloplacha.2018.07.004, 2018.

Keil, D. E., Buck, B., Goossens, D., Teng, Y., Pollard, J., McLaurin, B., Gerads, R. and DeWitt, J.: Health effects from exposure to atmospheric mineral dust near Las Vegas, NV, USA, Toxicol. Reports, 3, 785–795, doi:10.1016/j.toxrep.2016.09.009, 2016.

Kim, S., Park, S. and Lee, J.: Evaluation of performance of inexpensive laser based PM2.5 sensor monitors for typical indoor and outdoor hotspots of South Korea, Appl. Sci., 9(9), doi:10.3390/app9091947, 2019.

https://doi.org/10.5194/acp-2021-429
Preprint. Discussion started: 7 September 2021

Atmospheric Chemistry and Physics Discussions

Knippertz, P. and Stuut, J. B. W.: Mineral dust: A key player in the earth system., 2014.

Kurniawati, S., Santoso, M., Lestiani, D. D., Atmodjo, D. P. D., Sari, D. K. and Kusmartini, I.: Identification of Potential Source Location of Sulfur at Urban Area Bandung using Conditional Probability Function (CPF), IOP Conf. Ser. Earth Environ. Sci., 303(1), doi:10.1088/1755-1315/303/1/012042, 2019.

Li, Z., Guo, J., Ding, A., Liao, H., Liu, J., Sun, Y., Wang, T., Xue, H., Zhang, H. and Zhu, B.: Aerosol and boundary-layer interactions and impact on air quality, Natl. Sci. Rev., 4(6), 810–833, doi:10.1093/nsr/nwx117, 2017.

Loodin, N.: Aral Sea: an environmental disaster in twentieth century in Central Asia, Model. Earth Syst. Environ., 6(4), 2495–2503, doi:10.1007/s40808-020-00837-3, 2020.

Mahovic, N. S., Prieto, J., Jericevic, A., Gasparac, G. and Smiljanic, I.: EUMETSAT Webpage, [online] Available from: https://www.eumetsat.int/aralkum-desert-dust-pollutes-air-south-east-europe (Accessed 26 April 2021), 2020.

Manney, G. L., Livesey, N. J., Santee, M. L., Froidevaux, L., Lambert, A., Lawrence, Z. D., Millán, L. F., Neu, J. L., Read, W. G., Schwartz, M. J. and Fuller, R. A.: Record-Low Arctic Stratospheric Ozone in 2020: MLS Observations of Chemical Processes and Comparisons With Previous Extreme Winters, Geophys. Res. Lett., 47(16), doi:10.1029/2020GL089063, 2020.

Marécal, V., Peuch, V. H., Andersson, C., Andersson, S., Arteta, J., Beekmann, M., Benedictow, A., Bergström, R., Bessagnet, B., Cansado, A., Chéroux, F., Colette, A., Coman, A., Curier, R. L., Van Der Gon, H. A. C. D., Drouin, A., Elbern, H., Emili, E., Engelen, R. J., Eskes, H. J., Foret, G., Friese, E., Gauss, M., Giannaros, C., Guth, J., Joly, M., Jaumouillé, E., Josse, B., Kadygrov, N., Kaiser, J. W., Krajsek, K., Kuenen, J., Kumar, U., Liora, N., Lopez, E., Malherbe, L., Martinez, I., Melas, D., Meleux, F., Menut, L., Moinat, P., Morales, T., Parmentier, J., Piacentini, A., Plu, M., Poupkou, A., Queguiner, S., Robertson, L., Rouïl, L., Schaap, M., Segers, A., Sofiev, M., Tarasson, L., Thomas, M., Timmermans, R., Valdebenito, Van Velthoven, P., Van Versendaal, R., Vira, J. and Ung, A.: A regional air quality forecasting system over Europe: The MACC-II daily ensemble production, Geosci. Model Dev., 8(9), 2777–2813, doi:10.5194/gmd-8-2777-2015, 2015.

Marinoni, A., Cristofanelli, P., Calzolari, F., Roccato, F., Bonafè, U. and Bonasoni, P.: Continuous measurements of aerosol physical parameters at the Mt. Cimone GAW Station (2165 m asl, Italy), Sci. Total Environ., 391(2–3), 241–251, doi:10.1016/j.scitotenv.2007.10.004, 2008.

Masic, A., Bibic, D., Pikula, B., Blazevic, A., Huremovic, J. and Zero, S.: Evaluation of optical particulate matter sensors under realistic conditions of strong and mild urban pollution, Atmos. Meas. Tech., 13(12), 6427–6443, doi:10.5194/amt-13-6427-2020, 2020.

https://doi.org/10.5194/acp-2021-429
Preprint. Discussion started: 7 September 2021


Atmospheric Chemistry and Physics Discussions

Mie, G.: Beiträge zur Optik trüber Medien, speziell kolloidaler Metallösungen, Ann. Phys., 330(3), 377–445, doi:10.1002/andp.19083300302, 1908.

NASA: AERONET Inversion Products, Weather, 1–6, 2006.

National Centers for Environmental Prediction/National Weather Service/NOAA/US Department of Commerce: NCEP GFS 0.25 Degree Global Forecast Grids Historical Archive, , doi:https://doi.org/10.5065/D65D8PWK, 2015.

Okin, G. S., Mahowald, N., Chadwick, O. A. and Artaxo, P.: Impact of desert dust on the biogeochemistry of phosphorus in terrestrial ecosystems, Global Biogeochem. Cycles, 18(2), doi:10.1029/2003GB002145, 2004.

Pandolfi, M., Tobias, A., Alastuey, A., Sunyer, J., Schwartz, J., Lorente, J., Pey, J. and Querol, X.: Effect of atmospheric mixing layer depth variations on urban air quality and daily mortality during Saharan dust outbreaks, Sci. Total Environ., 494–495, 283–289, doi:10.1016/j.scitotenv.2014.07.004, 2014.

Prather, K. A., Wang, C. C. and Schooley, R. T.: Reducing transmission of SARS-CoV-2: Masks and testing are necessary to combat asymptomatic spread in aerosols and droplets, Science (80-.)., 368(6498), 1422–1424, doi:10.1126/science.abc6197, 2020.

Prospero, J. M., Ginoux, P., Torres, O., Nicholson, S. E. and Gill, T. E.: Environmental characterization of global sources of atmospheric soil dust identified with the Nimbus 7 Total Ozone Mapping Spectrometer (TOMS) absorbing aerosol product, Rev. Geophys., 40(1), 2-1-2–31, doi:10.1029/2000RG000095, 2002.

Rashki, A., Kaskaoutis, D. G. and Sepehr, A.: Statistical evaluation of the dust events at selected stations in Southwest Asia: From the Caspian Sea to the Arabian Sea, Catena, 165, 590–603, doi:10.1016/j.catena.2018.03.011, 2018.

Renard, J.-B., Dulac, F., Berthet, G., Lurton, T., Vignelles, D., Jégou, F., Tonnelier, T., Jeannot, M., Couté, B., Akiki, R., Verdier, N., Mallet, M., Gensdarmes, F., Charpentier, P., Mesmin, S., Duverger, V., Dupont, J.-C., Elias, T., Crenn, V. and Sciare, D.: LOAC: a small aerosol optical particle counter/sizer for ground-based and balloon measurements of the size distribution and nature of atmospheric particles-Part 1: Principle of measurements and instrument evaluation, Atmos. Meas. Tech., 9, 1721–1742, doi:10.5194/amt-9-1721-2016, 2016a.

Renard, J. B., Dulac, F., Berthet, G., Lurton, T., Vignelles, D., Jégou, F., Tonnelier, T., Jeannot, M., Couté, B., Akiki, R., Verdier, N., Mallet, M., Gensdarmes, F., Charpentier, P., Mesmin, S., Duverger, V., Dupont, J. C., Elias, T., Crenn, V., Sciare, J., Zieger, P., Salter, M., Roberts, T., Gobbi, M., Hamonou, E., Olafsson, H., Dagsson-Waldhauserova, P., Camy-Peyret, C., Mazel, C., Décamps, T., Piringer, M., Surcin, J. and Daugeron, D.: LOAC: A small aerosol optical counter/sizer for ground-based and balloon measurements of the size distribution and nature of atmospheric particles-Part 1: Principle of measurements and instrument

evaluation, Atmos. Meas. Tech., 9(4), 1721–1742, doi:10.5194/amt-9-1721-2016, 2016b.

Renard, J. B., Dulac, F., Berthet, G., Lurton, T., Vignelles, D., Jégou, F., Tonnelier, T., Jeannot, M., Couté, B., Akiki, R., Verdier, N., Mallet, M., Gensdarmes, F., Charpentier, P., Mesmin, S., Duverger, V., Dupont, J. C., Elias, T., Crenn, V., Sciare, J., Zieger, P., Salter, M., Roberts, T., Giacomoni, J., Gobbi, M., Hamonou, E., Olafsson, H., Dagsson-Waldhauserova, P., Camy-Peyret, C., Mazel, C., Décamps, T., Piringer, M., Surcin, J. and Daugeron, D.: LOAC: A small aerosol optical counter/sizer for ground-based and balloon measurements of the size distribution and nature of atmospheric particles-Part 2: First results from balloon and unmanned aerial vehicle flights, Atmos. Meas. Tech., 9(8), 3673–3686, doi:10.5194/amt-9-3673-2016, 2016c.

Rolph, G., Stein, A. and Stunder, B.: Real-time Environmental Applications and Display sYstem: READY, Environ. Model. Softw., 95, 210–228, doi:10.1016/j.envsoft.2017.06.025, 2017.

Sajani, S. Z., Miglio, R., Bonasoni, P., Cristofanelli, P., Marinoni, A., Sartini, C., Goldoni, C. A., De Girolamo, G. and Lauriola, P.: Saharan dust and daily mortality in Emilia-Romagna (Italy), Occup. Environ. Med., 68(6), 446–451, doi:10.1136/oem.2010.058156, 2011.

Sajani, S. Z., Bonasoni, P., Cristofanelli, P., Marinoni, A. and Lauriola, P.: Only coarse particles from the sahara?, Epidemiology, 23(4), 642–643, doi:10.1097/EDE.0b013e318258c23f, 2012.

Salvador, P., Molero, F., Fernandez, A. J., Tobías, A., Pandolfi, M., Gómez-Moreno, F. J., Barreiro, M., Pérez, N., Marco, I. M., Revuelta, M. A., Querol, X. and Artíñano, B.: Synergistic effect of the occurrence of African dust outbreaks on atmospheric pollutant levels in the Madrid metropolitan area, Atmos. Res., 226, 208–218, doi:10.1016/j.atmosres.2019.04.025, 2019.

Schepanski, K.: Transport of mineral dust and its impact on climate, Geosci., 8(5), doi:10.3390/geosciences8050151, 2018.

Sharma, A., Huang, H. P., Zavialov, P. and Khan, V.: Impact of Desiccation of Aral Sea on the Regional Climate of Central Asia Using WRF Model, Pure Appl. Geophys., 175(1), 465–478, doi:10.1007/s00024-017-1675-y, 2018.

Shen, H., Abuduwaili, J., Samat, A. and Ma, L.: A review on the research of modern aeolian dust in Central Asia, Arab. J. Geosci., 9(13), doi:10.1007/s12517-016-2646-9, 2016.

Shi, W., Wang, M. and Guo, W.: Long-term hydrological changes of the Aral Sea observed by satellites, J. Geophys. Res. Ocean., 119(6), 3313–3326, doi:10.1002/2014JC009988, 2014.

Šikoparija, B.: Desert dust has a notable impact on aerobiological measurements in Europe, Aeolian Res., 47, doi:10.1016/j.aeolia.2020.100636, 2020.

https://doi.org/10.5194/acp-2021-429
Preprint. Discussion started: 7 September 2021


Atmospheric Chemistry and Physics Discussions

SNPA: Sistema Nazionale Protezione Ambiente (SNPA) Webpage, [online] Available from: https://www.snpambiente.it/2020/03/31/polveri-dal-mar-caspio-allitalia/ (Accessed 26 April 2021), 2020.

Soupiona, O., Papayannis, A., Kokkalis, P., Foskinis, R., Sánchez Hernández, G., Ortiz-Amezcua, P., Mylonaki, M., Papanikolaou, C. A., Papagiannopoulos, N., Samaras, S., Groß, S., Mamouri, R. E., Alados-Arboledas, L., Amodeo, A. and Psiloglou, B.: EARLINET observations of Saharan dust intrusions over the northern Mediterranean region (2014-2017): Properties and impact on radiative forcing, Atmos. Chem. Phys., 20(23), 15147–15166, doi:10.5194/acp-20-15147-2020, 2020.

Stafoggia, M., Zauli-Sajani, S., Pey, J., Samoli, E., Alessandrini, E., Basagaña, X., Cernigliaro, A., Chiusolo, M., Demaria, M., Díaz, J., Faustini, A., Katsouyanni, K., Kelessis, A., Linares, C., Marchesi, S., Medina, S., Pandolfi, P., Pérez, N., Querol, X., Randi, G., Ranzi, A., Tobias, A., Forastiere, F., Angelini, P., Berti, G., Bisanti, L., Cadum, E., Catrambone, M., Davoli, M., de Donato, F., Gandini, M., Grosa, M., Ferrari, S., Pelosini, R., Perrino, C., Pietrodangelo, A., Pizzi, L., Poluzzi, V., Priod, G., Rowinski, M., Scarinzi, C., Stivanello, E., Dimakopoulou, K., Elefteriadis, K., Maggos, T., Michalopoulos, N., Pateraki, S., Petrakakis, M., Rodopoulou, S., Sypsa, V., Agis, D., Artiñano, B., Barrera-Gómez, J., de la Rosa, J., Diaz, J., Fernandez, R., Jacquemin, B., Karanasiou, A., Ostro, B., Salvador, P., Sanchez, A. M., Sunyer, J., Bidondo, M., Declercq, C., Le Tertre, A., Lozano, P., Pascal, L. and Pascal, M.: Desert dust outbreaks in Southern Europe: Contribution to daily PM10 concentrations and short-term associations with mortality and hospital admissions, Environ. Health Perspect., 124(4), 413–419, doi:10.1289/ehp.1409164, 2016.

Stein, A. F., Draxler, R. R., Rolph, G. D., Stunder, B. J. B., Cohen, M. D. and Ngan, F.: Noaa's hysplit atmospheric transport and dispersion modeling system, Bull. Am. Meteorol. Soc., 96(12), 2059–2077, doi:10.1175/BAMS-D-14-00110.1, 2015.

Tositti, L., Riccio, A., Sandrini, S., Brattich, E., Baldacci, D., Parmeggiani, S., Cristofanelli, P. and Bonasoni, P.: Short-term climatology of PM10 at a high altitude background station in southern Europe, Atmos. Environ., 65, 142–152, doi:10.1016/j.atmosenv.2012.10.051, 2013.

Tositti, L., Brattich, E., Masiol, M., Baldacci, D., Ceccato, D., Parmeggiani, S., Stracquadanio, M. and Zappoli, S.: Source apportionment of particulate matter in a large city of southeastern Po Valley (Bologna, Italy), Environ. Sci. Pollut. Res., 21(2), 872–890, 2014.

Varga, G., Kovács, J. and Újvári, G.: Analysis of Saharan dust intrusions into the Carpathian Basin (Central Europe) over the period of 1979-2011, Glob. Planet. Change, 100, 333–342, doi:10.1016/j.gloplacha.2012.11.007, 2013.

Washington, R., Todd, M., Middleton, N. J. and Goudie, A. S.: Dust-storm source areas determined by the total ozone monitoring spectrometer and surface observations, Ann. Assoc. Am. Geogr., 93(2), 297–313, doi:10.1111/1467-8306.9302003, 2003.

https://doi.org/10.5194/acp-2021-429
Preprint. Discussion started: 7 September 2021

Atmospheric Chemistry and Physics Discussions

WHO for European: Air Quality Guidelines, Air Qual. Guidel., 2006.

Zhang, X. X., Claiborn, C., Lei, J. Q., Vaughan, J., Wu, S. X., Li, S. Y., Liu, L. Y., Wang, Z. F., Wang, Y. D., Huang, S. Y. and Zhou, J.: Aeolian dust in Central Asia: Spatial distribution and temporal variability, Atmos. Environ., 238, doi:10.1016/j.atmosenv.2020.117734, 2020.

https://doi.org/10.5194/acp-2021-429
Preprint. Discussion started: 7 September 2021

Atmospheric Chemistry and Physics Discussions

820 **Appendix A**

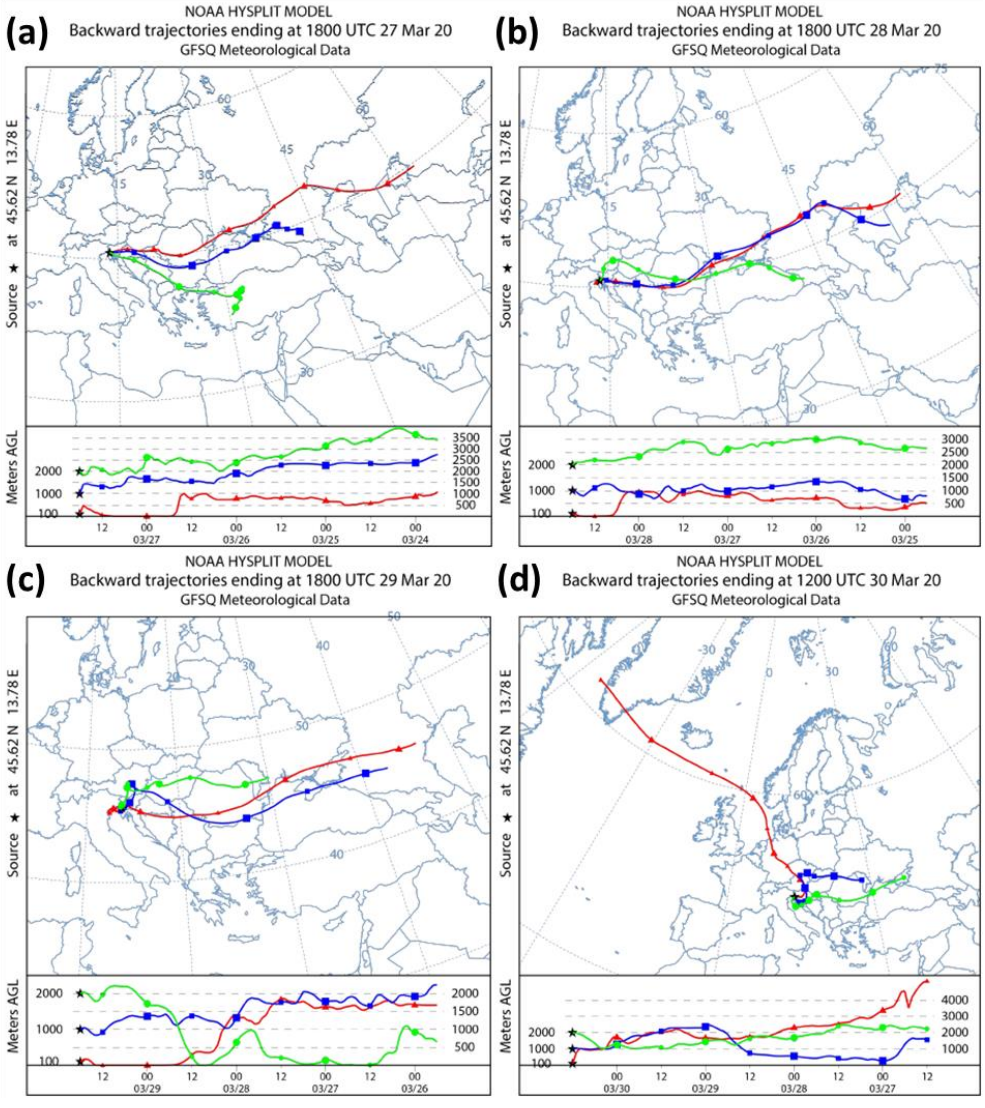

Figure A1. Back-trajectories (96-h backwards) ending at Trieste on a) 27 March 18:00 UTC; b) 28 March 12:00 UTC; c) 29 March 18:00 UTC; d) 30 March 12:00 UTC

https://doi.org/10.5194/acp-2021-429
Preprint. Discussion started: 7 September 2021

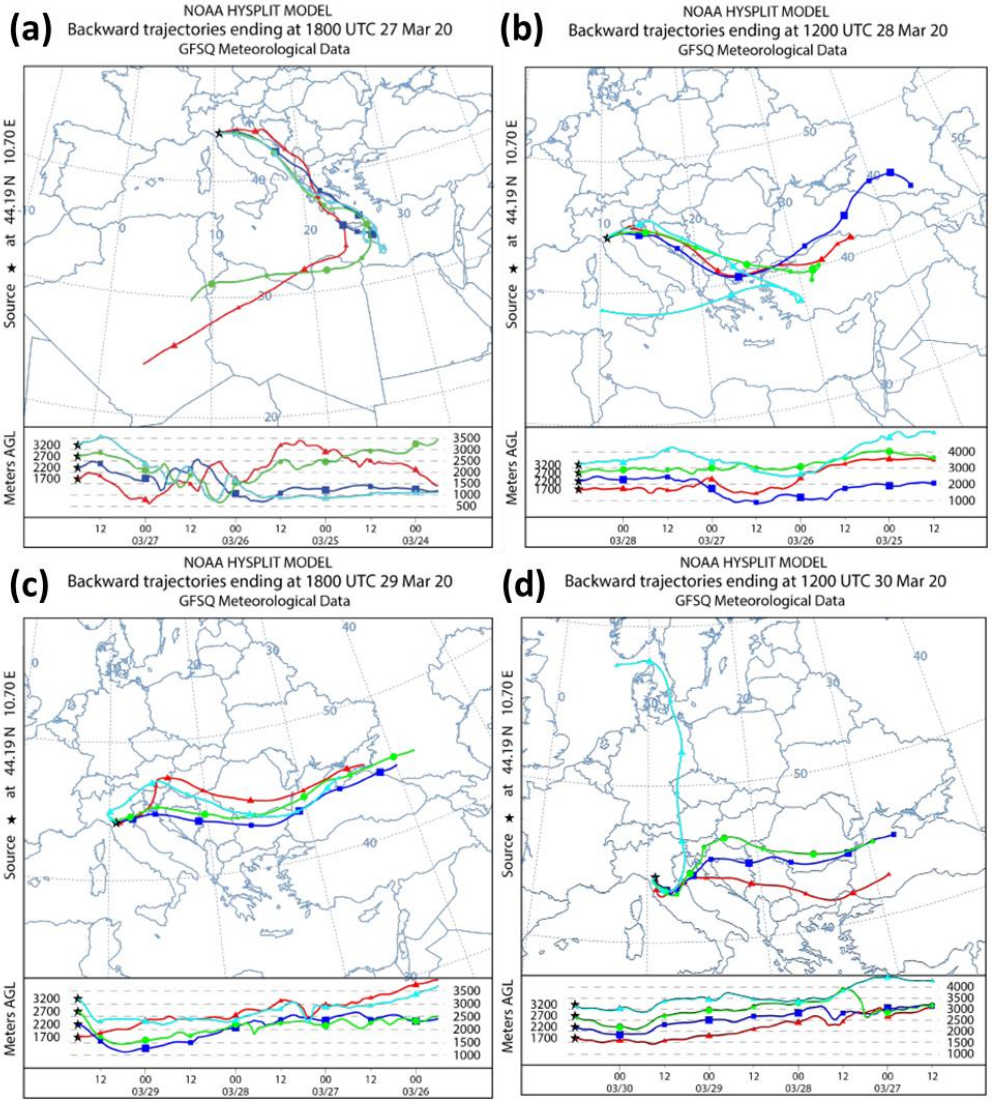

825 **Figure A2**. Back-trajectories (96-h backwards) ending at Mt. Cimone on a) 27 March 18:00 UTC; b) 28 March 12:00 UTC; c) 29 March 18:00 UTC; d) 30 March 12:00 UTC

https://doi.org/10.5194/acp-2021-429
Preprint. Discussion started: 7 September 2021

Atmospheric Chemistry and Physics Discussions

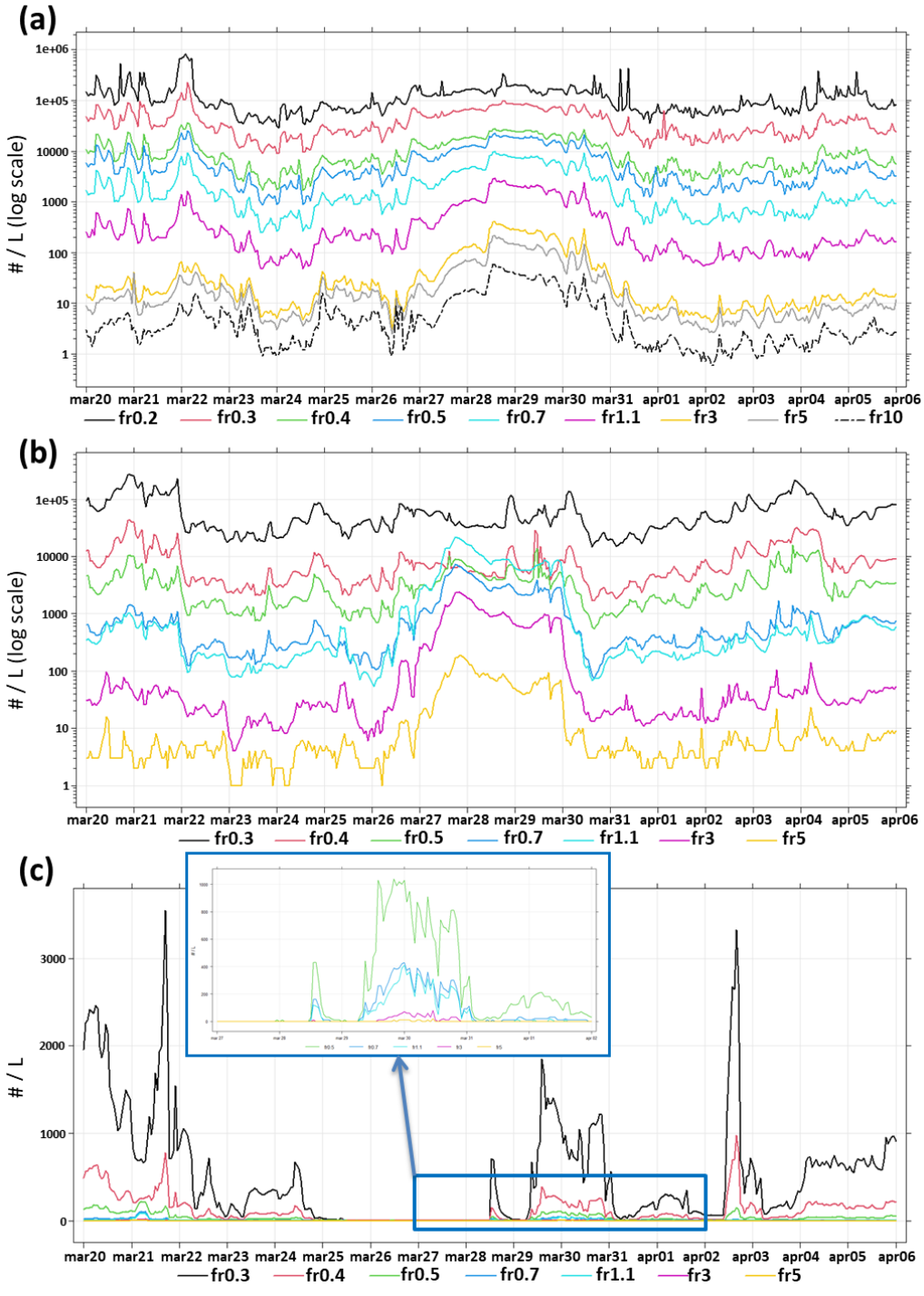

https://doi.org/10.5194/acp-2021-429
Preprint. Discussion started: 7 September 2021

Atmospheric Chemistry and Physics Discussions

Figure A3. Temporal trends of all fractions for the three OPCs: a) LOAC (Bologna); b) FAI (Trieste); c) Mt. Cimone (the blue rectangle shows a zoom on coarser fractions). For BO and TS, values are reported on a logarithmic scale. Values are in Counts dm^{-3} (# L^{-1})

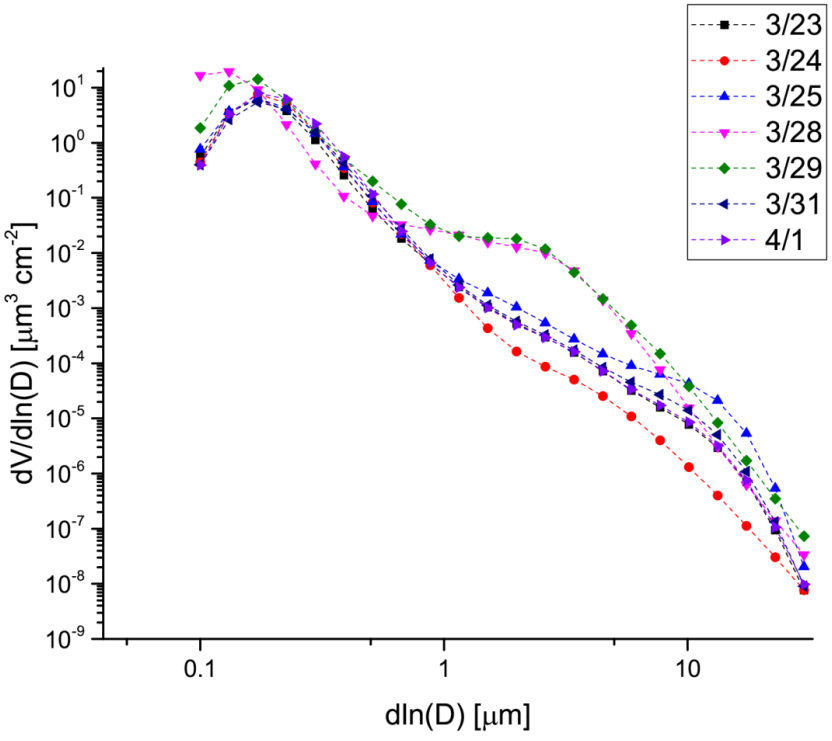

Figure A4. Volumetric size distributions retrieved by the inversion algorithm on days prior (23, 24 and 25 March), during (28 and 29 March), and after (31 March and 1 April) the arrival of the Caspian dust at the Venice AERONET site.